EUROPEAN SPALLATION SOURCE

MXType.Localized	
Document Number	MXName
Project Name	HEIMDAL
Date	30/03/2014
Revision	MXRevision MXPrinted Version
State	MXCurrent

ESS Instrument Construction Proposal
HEIMDAL

Please read the call for instrument proposals found at europeanspallationsource.se/instruments2013 and the "Preparation and Review of an Instrument Construction Proposal" to guide you in preparing your instrument construction proposal.

	Name (name, title, e-mail address)	**Affiliation** (name of institution, address)
Proposer	Mogens Christensen, Assoc. Prof. mch@chem.au.dk	Center for Materials Crystallgraphy iNANO & Department of Chemistry Aarhus University DK-8000 Aarhus
Co-proposers	Kim Lefmann, Assoc. Prof. lefmann@nbi.dk Sonja Lindahl Holm Sonja@fys.ku.dk Mads Bertelsen mads.bertelsen@gmail.com Jürg Schefer, Head of Neutron Diffraction juerg.schefer@psi.ch Poul Norby, Senior Scientist, pnor@dtu.dk	Niels Bohr Institutet, Universitetsparken 5, DK-2100 København Ø Laboratory for Neutron Scattering Paul Scherrer Institut CH-5232 Villigen PSI Technical University of Denmark Building 229, room 120 DK-4000 Roskilde
ESS coordinator	Paul Henry	European Spallation Source ESS AB Box 176 S-221 00 Lund

Note: All proposals received by ESS will be included as Expressions of Interest for In-kind contributions. ESS will use this information for planning purposes and the proposer or affiliated organization is not obligated to materially contribute to the project.

The following table is used to track the ESS internal distribution of the submitted proposal.

	Name
Document submitted to	Ken Andersen
Distribution	Dimitri Argyriou, Oliver Kirstein, Arno Hiess, Robert Connatser, Sindra Petersson Årsköld, Richard Hall-Wilton, Phillip Bentley, Iain Sutton, Thomas Gahl, relevant STAP

ENCLOSURES

Letter of interest – Dominik Schaniel (Université Lorraine)
Letter of interest – Bjørn Hauback (IFE)
Letter of interest – Daniel Urffer (Saint-Gobain)
Letter of interest – Petr Novák (PSI)
Appendix A – Extended Science Case
Appendix B - Comparison of Multiscale Instruments
Appendix C - Sample environment consideration
Appendix D – HEIMDAL – A high resolution powder diffractometer
Appendix E- pancake moderator effects

EXECUTIVE SUMMARY [1-2 PAGES]

Advances in material science come through an in-depth understanding of the relationships between structure and properties. Profound insights into these relationships are a common goal across condensed matter science, from high precision crystallographic studies to kinetics studies, and are a prerequisite for the rational design of new and improved materials. Traditionally, materials have been studied at equilibrium far from operating conditions – but there is now a growing effort to investigate materials under more realistic conditions and on multiple length scales. To a large extent the interest in multiple length scales has been driven by new developments at synchrotron sources. Here, we propose an instrument combining state-of-the-art thermal neutron powder diffraction (TNPD), small angle neutron scattering (SANS) and neutron imaging (NI) with the goal of studying *real* materials, in *real* time, under *real* conditions. Neutrons are the ideal probe for *in situ* and *in oprandi* studies. However, no neutron instrument capable of covering multiple length scales in real time exists today.

The long pulse at ESS is, at first glance, not ideal for building powder diffraction instruments. The requirements for a powder diffractometer are good peak resolution and large reciprocal space coverage, which is normally obtained by short pulses and short wavelength neutrons. However, a pulse-shaping chopper can provide a short well defined pulse at the expense of flux and a long distance between the moderator and the sample then provides high resolution. This results in narrow wavelength band, which can be chosen to coincide with the relatively narrow high-brilliance pulse produced by the thermal moderator. The intrinsic problems of a narrow wavelength band powder diffractometer can be thus minimized by collecting data in 2D both as function of angle and time.

HEIMDAL is designed to use a narrow wavelength band coinciding with the maximum brightness from the thermal moderator. The pulse-shaping chopper controls the pulse length and facilitates both high-resolution (short pulse, lower intensity) and high-rate (long pulse, lower resolution) data collection. Conventional facilities typically have to build both a high resolution *and* a high flux instrument. At ESS it is possible to have *both functionalities in a single instrument*. A significant benefit of the HEIMDAL design is the simple peak profile functions describing the data, due to the relatively simple chopper system and the cylindrical detector geometry. The high angular coverage and relatively short wavelength will allow

collection of data suitable for low-resolution pair distribution function (PDF) analysis. Additional backscattering detectors are installed to improve statistics at high *q* and compensate for the low flux of the shortest wavelength neutrons.

In addition to the optimized TNPD setup, HEIMDAL is designed with the added capabilities of SANS and NI. A large spatial coverage is crucial because understanding advanced functional materials often involves understanding their response to external stimuli such as gas flow, pressure, or temperature, which can be difficult to recreate exactly in subsequent experiments. A classic example is heterogeneous catalysts, which depend on the atomic structure of catalytic nanocrystallites in a microporous matrix. All length scales are relevant for the efficiency of the catalytic process; therefore, in-depth knowledge into the structure and functionality requires multiple length scale coverage with sufficiently good time resolution. Commonly, data on different length scales are collected separately and quite often in the equilibrium state, *i.e.*, *after* the external stimuli have been applied.

Our ambition is to build a state-of-the-art instrument combining NPD, SANS and NI in a single uncompromised setup: NPD covering the atomic regime from 0.01 to 5 nm; SANS surveying the nanometer regime from 2-100 nm; and NI revealing structural features in direct space from 0.05-50 mm. The total length scale coverage thus spans 9 orders of magnitude. The name HEIMDAL comes from the Norse god guarding the rainbow bridge between the world of men and gods, who was said to have an extraordinarily good senses of seeing and hearing

The experimental techniques of NPD, SANS, and NI have highly different requirements in terms of the incoming neutron beam. Therefore, all existing instruments covering broad length scales are focused towards either SANS or NPD while sacrificing the other (e.g., NOVA, i-Materia, HI-SANS at J-Parc or NIMROD at ISIS). BEER at ESS is also foreseen to combine NPD and SANS; however, this instrument is dedicated to a completely different user community, namely engineering. We propose an entirely novel concept, where two independent guides view the cold and thermal moderators, respectively. The two beams are extracted from the same beamport, and can be individually optimized without sacrificing the capability of either techniques..

Initially HEIMDAL will be operated as thermal neutron powder diffractometer, for both the high-resolution and the *in situ* user communities. However, when HEIMDAL is completed it will be capable of combined TNPD/SANS/NI experiments. The completed instrument will attract a new user community, rapidly growing in the X-ray world, that has begun studying materials at multiple length scales following the development of dedicated SAXS/WAXS (small angle X-ray scattering/wide angle x-ray scattering) beamlines at new synchrotron sources. The proposed multiple length scale neutron instrument HEIMDAL will be a game-changer in neutron scattering because it will provide new capabilities for investigating multiple dimensions at fast time scales. Topics of particular interest are materials containing light elements, related to energy, composites, matrix embedded systems, phase transition and nucleation and magnetic material – in other words, **the materials of the future.**

TABLE OF CONTENTS

ENCLOSURES **2**

Executive Summary [1-2 Pages] **2**

Table of ContentS **2**

1. Instrument Proposal [app. 20 pages] **4**

1.1 Scientific Case [5 pages] 4

1.2 Description of Instrument Concept and Performance [10 pages] 14

1.3 Costing and maturity[2 pages] 28

2. List of Abbreviations **38**

1. INSTRUMENT PROPOSAL [APP. 20 PAGES]

1.1 Scientific Case [5 pages]

Functional materials have always been a major driver of civilizations in their search for prosperity and superiority. This is reflected by names associated with different periods in history: the Stone Age, the Bronze Age, the Iron Age etc. Today, it can be argued that we are approaching the end of the Silicon Age, as we reach the density limit for transistors on chips. Research efforts have continuously developed new functional materials to extend Moore's law beyond the practical limits of silicon.[1] The "hot topics" in science for 2025 and beyond are hard to predict, but new functional materials are certain to play a key role. Finding and characterizing these new materials are the responsibility of material scientists, solid-state chemists and condensed-matter physicists. HEIMDAL is focused on these communities, with their common goal of relating structural understanding to physical properties. An ever-increasing number of neutron diffraction studies are parametric studies, where investigations are carried out as function of, e.g., temperature, pressure and magnetic field. Recent instruments have sufficient flux to collect data as function of time. The long guide and full angular detector coverage of HEIMDAL will make the instrument ideal for carrying out time-resolved studies with high q-resolution for accurate structure determination. Studies of functional materials are generally shifting from data obtained in the equilibrium state, to experiments performed *in situ* and *in operandi*.

HEIMDAL is an optimized thermal-neutron powder diffractometer (TNPD). The chopper setup of HEIMDAL allows the instrument to be run in a high-flux mode for fast data acquisition, or in a high-resolution mode for very precise crystallographic studies of complicated structures. The broad q-range coverage of 0.6-21 $Å^{-1}$ allows the precise determination of atomic displacement parameters and may even be used for low-resolution pair distribution function (PDF) analysis.

HEIMDAL is designed with a relatively open sample geometry that allows the use of bulky cryostats, magnets and pressure cells without shadowing any part of the detectors. The detectors are placed in a cylindrical disposition around the sample and cover ±18° of the horizontal plane. This setup allows effective use of a radial collimator to reduce background from the sample environment. The open geometry and effective background reduction allow

users to bring their own experimental setups to the instrument. Space will be allocated near the instrument to allow a sample environment to be set up while the previous experiment is still running, reducing the required changeover time. This design permits long-term experiments where sample are held under certain conditions to be measured periodically.

In other words, HEIMDAL appeals to a vast user community of chemists and physicists interested in problems ranging from pair distribution function (PDF) analysis to classical high-resolution crystallography, However, HEIMDAL's greatest potential is for time-resolved investigations, where the instrument's length permits it to use a large fraction of the long pulse provided by the ESS. There is a growing community of material scientists interested in following processes as function of time. We believe that in years to come the demand for performing *in situ* studies will also included a request for covering multiple length scales. If we wish to understand and improve functional materials it is paramount to understand the structure at all length scales and with sufficient time resolution to follow physical and chemical processes. Until now, different length scale information is collected separately and quite often *post mortem i.e.* after the process has taken place. Such experiments allow scientists to make educated guesses. HEIMDAL is designed to include an option extending the length scale coverage of TPND into those of small angle neutron scattering (SANS) and neutron imaging (NI). TNPD combined with SANS and NI capabilities allows quasi-simultaneous coverage of length scales from 0.01 nm to 50 mm, spanning more than 9 orders of magnitude. Its design uses a single beamport to extract a cold and a thermal beam. Combining TNPD, SANS and NI in a single instrument allows studying multiple length scales simultaneously and obtaining information on the atomic-, nano-, meso-, and microstructure scale.

HEIMDAL will serve the conventional powder diffraction community both in its desire for both resolution and speed, while spawning an entirely new user community focused on its new capabilities for multiple length scale studies.

The scientific focus areas of the instrument are related to the strengths of neutron scattering in comparison with X-ray scattering: contrast between elements with similar Z; magnetic materials; use of bulky sample environment; and measurements of samples in the sizes required for real applications. The research areas in which HEIMDAL will excel can be divided into four different groups - all to a large extendt involving *in situ* investigations:

- Light elements and energy related materials
- Composites, scaffolds or matrix embedded systems
- Phase transition and nucleation
- Materials with magnetic properties

These topics map very well onto the science case written into the ESS Technical Design Report (TDR). A wider perspective on *in situ* investigations and science cases can be found in Appendix A. The instrument design allows large q-coverage with a time resolution sufficient to follow chemical and physical processes in real time. HEIMDAL is designed to study **real materials**, in **real time**, and under **real conditions.**

1.1.1 Light elements and energy related materials:

Neutrons provide unique information about energy storage materials, which are becoming increasingly important as renewable energy takes over from conventional energy sources. Developing new materials may be the only solution to overcome the greenhouse effect/CO_2

problem.[2] Two elements are of particular interest in energy storage, namely lithium and hydrogen. Both of these are difficult to observe by X-ray scattering, due to their small number of electrons. Lithium is the key component in Li-ion batteries, whereas hydrogen is the active element in hydrogen storage materials. For neutron scattering these elements hold special potential as they have good contrast with respect to other elements. The ability to follow charge and discharge of batteries and hydrogen storage materials *in situ* is a crucial first step on the route to understanding and improving their properties.

Another area where energy research can benefit from neutron investigations is oxygen-containing compounds. Examples of applications of oxide materials are membranes for solid oxygen fuel cells (SOFC),[3] catalyst support materials, superconductors, ceramic filters, thermoelectric materials etc. Information about oxygen is difficult to extract from X-ray diffraction data when much heavier elements are present. In the case of neutron scattering, oxygen has a scattering length comparable to heavy elements.[4]

1.1.2 Composite, scaffold or matrix embedded systems

Hydrogen storage and Li-ion batteries can be considered as matrix-embedded systems, where the Li or H is placed in a host matrix from which it can be inserted or extracted. Other important compounds that can be represented as matrix-embedded systems include molecules in porous matrices, drug transport and magnetic materials. Hybrid materials, where inorganic and organic building blocks are distributed on the nanoscale, are also included in this group of materials.

Heterogeneous catalysts are likewise an example of hybrid materials, where nanocrystalline catalyst particles are embedded in a porous support matrix. Understanding these complex systems require knowledge about: i) the different lengths of the support matrix including pore volume and the embedded catalytic nanoparticles, together with their atomic structure; and ii) *in operandi* data of catalytic systems, which maps catalytic performance against external *stimuli* such as temperature, gas flow, concentration of fouling atoms, etc[5-7]. To improve the properties of catalysts, a good understanding of their behaviour under working conditions is essential. Time resolved data collection on catalytic materials is therefore highly important.

Photo-switchable molecules are another example of composite materials where molecules are embedded in a porous matrix.[8] They have potential applications as optical data storage materials or in cancer therapy, where they can be used to deliver radicals. Combining powder diffraction, SANS and imaging is crucial for extracting complete information about the pore size and structure of embedded molecules. These photo-switchable molecules are unstable and change over time, therefore it is essential to collect data at multiple length scales during the same experiment at the same time.

1.1.3 Phase transitions and nucleation

The capabilities of HEIMDAL for *in situ* studies permit important aspects of chemical synthesis to be followed, notably nucleation and the role metastable intermediate phases, as well as phase transitions upon variation of thermodynamic conditions such as temperature, pressure, volume, or composition. Metastable transitions are highly sensitive to the history of external *stimuli*, which can be difficult to control. *In situ* information is needed to determine the critical parameters for optimal synthesis conditions.

HEIMDAL will be of general interest when studying *in situ* chemistry, e.g. solid-state, liquid-to-solid-state, gas-to-solid-state, solvothermal and supercritical reactions[11-14]. A common feature of these syntheses is the presence of precrystalline states, where agglomerates form before they crystallize[14]. SANS and low-resolution total scattering can give information about the pre-crystalline state, while diffraction provides structural information in crystallization and growth state. Chemical synthesis has a broad fundamental science appeal. However, there are also examples with great technological importance such as the curing of cement[15-20] and the suppression of nucleation of clathrate hydrates in oil pipes[21-27]. These systems have already been extensively studied using neutron techniques, but so far those studies have been limited to either SANS, powder diffraction or NI. Combining all techniques to look at the same sample will provide much more profound information about how these processes evolve as function of time. Biologically inspired systems are also interesting from an *in situ* perspective, and many environmental and biomineralization processes occur on timescales accessible by HEIMDAL[9, 10].

In general, HEIMDAL is well suited for studying nucleation, growth and aging processes of multicomponent materials, including crystal growth and phase transitions caused by external stimuli such as temperature, pressure or magnetic field.

1.1.4 Materials with magnetic properties

Multiferroics have in recent years drawn increasing attention. These systems couple magnetism with either electrical, mechanical, thermal, or optical properties[28]. Multiferroics are of great technologic interest as they raise the possibility of controlling magnetic properties[29, 30] with an electrical field, pressure or *vice versa*[31]. Multiferroics include materials for spintronic applications[32, 33] where the aim is to manipulate spin domains in half-metallic ferromagnetic systems. Multiferroic properties can be realised in single-phase or composite materials. Topological ferroic systems are physical systems governed by domain structure[34, 35] - the topology of the domain wall being susceptible to chemical effects[36], size effects and magnetic interactions.

Examples of multi-length scale materials are the colossal magneto-resistance perovskite compounds[37]. These perovskites possess a metal-insulator transition and are susceptible to phase separation promoted by electron/hole doping *via* chemical substitution[38, 39]. Fundamental[40] and technological applications[41] rely on understanding the coupling of these different length scales and the degrees of freedom. Aging, phase transitions, percolation phenomena, defects mobility, phase homogeneity, domains wall pinning, atomic and magnetic structure are the keys parameters in the improvement of magneto-memory shape alloys[42], spintronics, magnetocaloric and magnetocapacitance materials[43]. Multidimensional length scales collected simultaneously as offered by HEIMDAL would greatly aid the understanding of this interesting class of materials. HEIMDAL will be able to tackle scientific challenges in this frontier area of science and identify magnetic properties more accurately especially *in operandi* for magnetic phase separation, quantum criticality in magnetic, superconductor materials, and ferroic/multiferroic systems[43], and high performance magnetic exchange-coupled materials[42].

1.1.5 User community: size and impact for existing and potential user

The long pulse at ESS allows the design of an instrument capable of high-resolution and high flux, simply by tuning the pulse-shaping choppers of the instrument. Figure 1 illustrates how different pulse length allows for different kind of experiments at the same instrument.

Current facilities typically have instruments designed for either high resolution or high flux. Examples for high-flux instruments are GEM/POLARIS@ISIS, iMateria@J-Parc, D20@ILL, and WOMBAT@ANSTO. The same facilities also have high-resolution instruments e.g. HRPD@ISIS, S-HRPD@J-Parc, D1A/D2B@ILL and ECHIDNA@ ANSTO. The fact that a single instrument at ESS can cover a broader science case does not mean that fewer instruments are need for the user community – only that the versatility of the different instrument will be higher. The demand for powder diffraction beamtime is generally high and oversubscription rates are typically around 2. The annual turnout of published papers from powder diffraction instruments is on average about 550 and the major topics are chemistry (including crystallography), physics and materials science. The use by the different disciplines can divided into a subset of instrumental requirements.

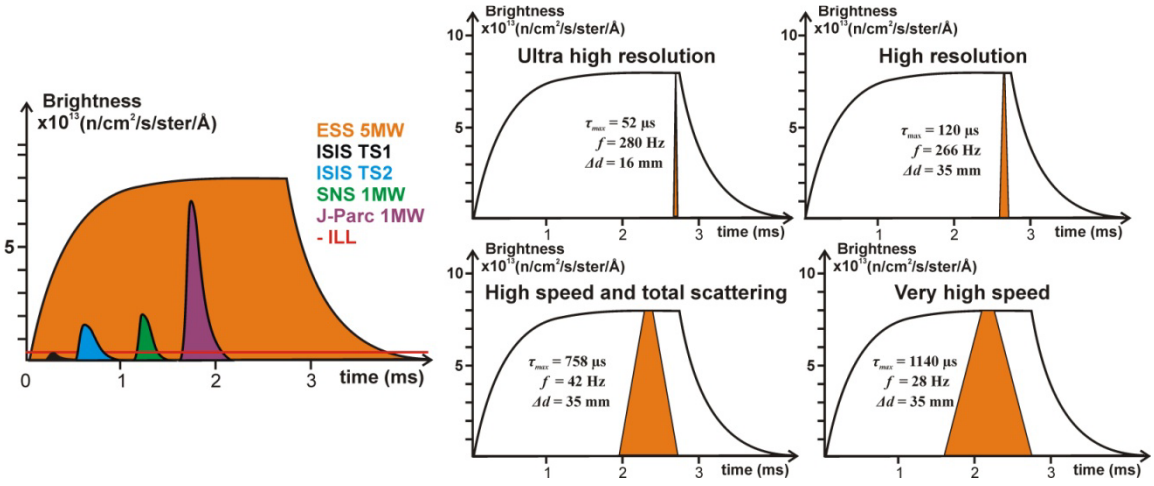

Figure 1: Comparison of pulse brightness at different facilities (left), and the pulse used for obtaining ultra high resolution, high resolution, high speed and very high speed with HEIMDAL@ESS.

High resolution powder diffraction:

High-resolution powder diffraction is aimed at accurate structure determination including lattice parameters, atomic coordinates, atomic displacement parameters and peak shape effects like strain and size. High-resolution structural characterisation is a classical crystallographic discipline linked to chemistry, physics and material science. The long source-to-sample distance of HEIMDAL allows very high resolution, by reducing the pulse width using the counter-rotating double choppers. HEIMDAL is capable of catering to a user community seeking high resolution. Unfortunately, high resolution comes at the cost of a reduced pulse width, therefore in high-resolution mode HEIMDAL will not take full advantage of the long pulse at ESS, see Figure 1.

In situ and high speed powder diffraction:

Interest in performing parametric and *in situ* studies is increasing, reflected in the commissioning of new powder diffraction instruments at facilities like the SNS, J-Parc and FRM-II, as well as instrument upgrades at, e.g., Kjeller and PSI. The desire to perform parametric and *in situ* studies is expressed by communities from materials science, physics, chemistry and crystallography. The speed with which HEIMDAL will be capable of collecting data will open up completely new opportunities for *in situ* and *in operandi* studies. The long distance between source and sample allows relatively good resolution for the long neutron

pulse, taking maximum advantage of the ESS. The open detector geometry of HEIMDAL allows flexible experimental conditions, which is a great advantage when performing *in situ* experiments as these often involve equipment supplied by the users. The user community for *in situ* and high-speed diffraction is foreseen to grow as completely new studies can be undertaken, studies hitherto unimaginable at weaker sources.

Total scattering and pair distribution function capabilities:

The detector coverage from 10 to 170° ensures data collection in a q-range from 0.6-21 $Å^{-1}$. This gives a maximum real-space resolution of $\Delta r = \pi/q_{max} \sim 0.15$ Å. A dedicated neutron instrument for total scattering goes to significantly higher q, but HEIMDAL's q-range is sufficient for the study of nanomaterials and disordered materials. Together with the possibility of a relaxed resolution for total scattering, the experiments can take full advantage of the long pulse at ESS in time-resolved total scattering experiments. Interest in pair distribution function (PDF) analysis is rapidly growing in the X-ray community partly due the availability of synchrotron light, and recent user-friendly software developments open the field to non-expert users. Both Bruker and PANalytical offer laboratory equipment capable of measuring data for PDF analysis using either Mo or Ag radiation. The wider use of total scattering in laboratory setups will inevitably expand this user community.

Combined powder diffraction and small angle scattering:

A unique feature of HEIMDAL is the foreseen combination of SANS and TNPD. The novel two-guide setup with cold and thermal neutrons allows the collection of uncompromised powder diffraction data, together with narrow-band SANS data. The instrument bridges the world of small-angle wide-angle scattering for the study of complex materials. While the user community for such an instrument may initially be limited, HEIMDAL will, in the long-term, attract a completely new user group interested in functional and composite materials. The combination of SANS and diffraction allows completely new science projects to be undertaken. At synchrotron sources, combined SAXS/WAXS studies are ramping up with more than 20 beamlines worldwide offering (and, in the case of the newer instruments, dedicated to) simultaneous SAXS/WAXS studies. It is expected that researchers in this user community will pose scientific questions soluble only with neutron scattering data.

Industrial users:

HEIMDAL will be of great interest to industrial users wishing to probe different length scales in commercial samples. HEIMDAL offers industry oriented groups a single point of entry for performing a broad range of experiments. Special care will be taken to allow an easy and transparent operation and data visualization for these non-expert users.

Complementarities to X-rays:

An X-ray powder diffraction and imaging beamline has been proposed for MAX-IV. This X-ray setup is highly complementary to the capabilities of HEIMDAL and great synergies between X-ray and neutron studies are expected, due to the proximity of the two instruments at ESS and MAX-IV.

In summary: HEIMDAL covers a science case from the distinct fields of crystallography, chemistry, physics and materials science for universities and industry. The focus will be on *in situ* and *in operandi* studies, where the length of HEIMDAL will take advantage of the long pulse at ESS. The high q-range coverage will allow low-resolution PDF experiments to be carried out. With the addition of SANS, HEIMDAL will be able to cover a uniquely broad length scale with a single instrumental setup.

1.1.6 Comparison with similar existing instruments:

The comparison is mainly focused at existing powder diffraction instruments. At the end of the section the SANS part will be briefly addressed.

Comparison of powder diffraction capabilities:

The design of HEIMDAL is aimed at best utilizing the long pulse at ESS, and the comparison will mainly focus at instruments for fast *in situ* measurements. Even so HEIMDAL has capabilities as a high resolution powder diffractometer. Comparison between different instruments is difficult, because many factors must be taken into account when considering speed of collecting data such as:

Time averaged flux at sample position (Φ)
Resolution ($\Delta d/d$)
Detector coverage (D_{area}) and detector efficiency (D_{eff})
Q-range
Sample volume
Background

The long pulse at ESS allows changing flux and resolution ($\Delta d/d$), and a comparison becomes even less meaningful. Table I gives a crude criterion using a gain factor G_{eff} for the comparison of existing instruments. The gain factor is defined as the product of **flux**, detector **coverage** and **efficiency** divided by the **resolution** $\Delta d/d$@90. The gain factor G_{eff} has been normalized to the performance of GEM@ISIS. A variation in the possible sample volume naturally scales directly with gain factor and is not taking into account.

Instrument	Type	$\Delta d/d$@90^0	Δλ (Å)	λ_{mean} (Å)	q_{range} (Å^{-1})	Detector Type	D_{area} (sr)	flux (n/s/cm^2)	G_{eff}
GEM @ ISIS	TOF	0.50%	3.5	1.8	0.04-100	Sc	3.9	2e6	**1**
New Polaris @ ISIS	TOF	0.50%	5.5	2.9	0.7-125	Sc	5.67	~1e7	**~7**
Nomad @ SNS	TOF	0.60%	3.0	1.6	0.5-125	^{3}He	4	~1e8	**~71**
PowGen @ SNS	TOF	0.50%	2	1.1	3-120	Sc	4.4	~2.5e7	**~14**
I-materia@JPARC	TOF	0.50%	6	3.3	0.007-70	^{3}He	4	~1e8	**~86**
Nova@JPARC	TOF	0.50%	7	3.6	0.4-100	^{3}He	5	~4e8	**~385**
D20@ILL	CW	1.6%	-	1.3	0.2-8	^{3}He	0.27	~1e8	**~2**
Powtex@FRM2	TOF	0.60%	1.4	1.6	0.4-13	^{10}B	6.2	~1e7	**~7**
Wombat@OPAL	CW	1.0%	-	2.4	0.4-4	^{3}He	0.59	~1.3e8	**~8**
HEIMDAL (high res.)	**TOF**	**0.17%**	**1.7**	**1.5**	**0.6-21**	**Sc**	**2.25**	**~3.8e6**	**~3**
HEIMDAL (Med res.)	**TOF**	**0.60%**	**1.7**	**1.5**	**0.6-21**	**Sc**	**2.25**	**~6.2e8**	**~150**
HEIMDAL (high flux)	**TOF**	**1.0%**	**1.7**	**1.5**	**0.6-21**	**Sc**	**2.25**	**~2.0e9**	**~290**

Table I Instrument comparison, the different values for flux etc. are found at web pages and papers are more through description of the individual instruments can be found in appendix B. The $G_{eff} = \Phi D_{area} D_{eff} / (\Delta d/d$@90°), the D_{eff} is set to 100% for ^{3}He and 60% for scintillation counters and ^{10}B.

At short pulsed spallation sources flux and resolution is to a large extend determined by the pulse characteristics and the instrument length. At ESS the pulse length can be chosen to match the speed of the experiment. HEIMDAL is designed to take advantage of the long

pulse and the resolution $\Delta d/d$@90° can be varied between 0.1% to 2% or $\Delta d/d$@170° between 0.015% to 1.5% for λ_{mean} =1.5 Å. The instrument is optimized with regards to divergence and pulse lengths of 121-758 µs, which gives a time averaged flux of ~$4 \cdot 10^6$-$2 \cdot 10^9$ n/s/cm^2. The calculations are described in larger detail in section 1.2 (Description of the instrument).

The flux on sample position can be varied by changing the speed of the pulse shaping chopper. By matching the beam divergence horizontally and vertically to the pulse length an increased flux can be obtained for longer pulse length. Figure 2 illustrates the tradeoff between resolution and flux.

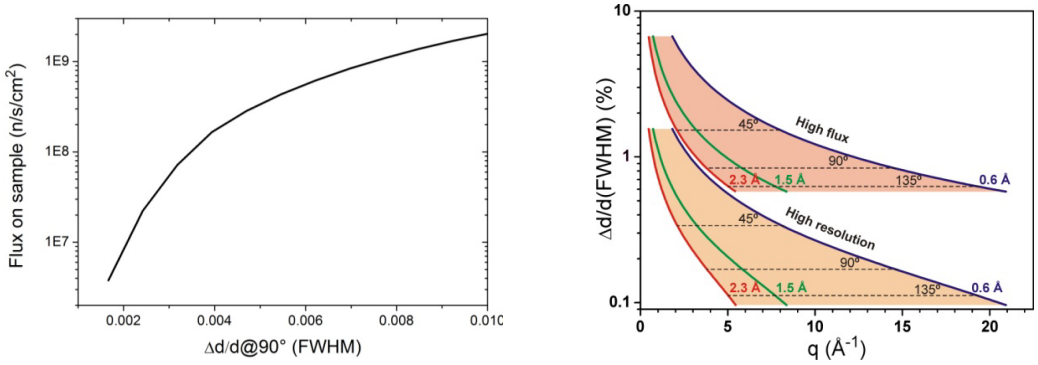

Figure 2 (left) flux on sample (n/s/cm^2) with constant size of 5x15 mm, the beam divergence and the pulse length can be match to change the flux by 2 orders of magnitude. (right) resolution as function of q. The figure also indicated the q-space coverage. The wavelengths shown are 0.6 Å (blue), 1.5 (green), and 2.3 Å (red).

Comparison and complementarities to other ESS instruments:

Currently, three other instruments are proposed with significant powder diffraction capabilities: POWHOW, MODI and BEER. POWHOW is a bispectral powder diffractometer using frame multiplication to include both thermal and cold neutrons for the data collection; it is designed to addressing large unit cells and magnetic materials, with possibilities for single crystal diffraction. POWHOW is about half the length compared to HEIMDAL, this allows POWHOW to extract a broader wavelength band, at the expense of a shorter pulse width for the same resolution. Therefore HEIMDAL can be tuned to have a higher flux and a better resolution for short wavelength neutrons, while POWHOW performs better for long wavelength neutrons. HEIMDAL and POWHOW have some overlap in the science case, as both can do high resolution and perform fast data collection. However, there are also clear complementarities HEIMDAL can perform low resolution total scattering experiments while POWHOW can address complicated magnetic structures and single crystal diffraction. Additionally HEIMDAL has the option for SANS to investigate samples over a wider size range. Finally HEIMDAL is designed with more flexible sample environment geometry permitting more complex sample environments to be installed.

The main driver for MODI is the possibility for discriminating incoherent background to perform measurements on hydrogenous samples, therefore there is no significant overlap between MODI and HIEMDAL. With regard to BEER at an initial glance the instrument may look alike, same length, both aspire to do *in situ* studies, and both suggest options for small angle scattering. But here the similarity ends: BEER has a completely different user community, namely materials engineering, there is practically no overlap between the

crystallographic oriented user community and the engineering user community. The difference is reflected in the chopper and detector setup. BEER has a complex chopper setup to allow for multiplexing, making multiple short pulses for following single diffraction peaks. Likewise the detector setup designed for following only few reflections. The sample space of BEER allows even more complicated and bulky sample environments compared to HEIMDAL.

Instrument performance:

Below is McStats simulations of HEIMDAL@ESS, these simulations represent high resolution and high flux at τ = 121 μs and 758 μs. The simulations can be compared to the simulations D20, POWGEN and POWHOW presented in the POWHOW proposal by Werner Schweika.

HEIMDAL – ESS McStats simulations, Mads Bertelsen and Sonja Holm
Sample: 0.3 cm^3, detector efficiency (assumed 100% no wavelength dependence), solid angle 1.8 sr, the backscattering detectors are not considered.
High resolution – flux: 3.8x10^6 n/s/cm^2 High speed – flux: 2.0x10^9 n/s/cm^2

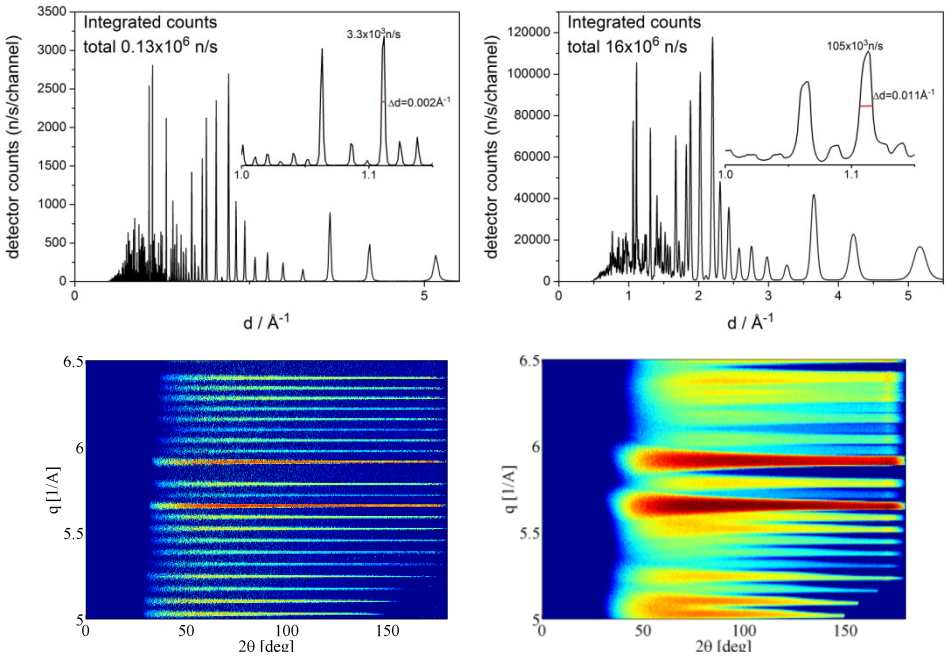

Figure 3: Comparison of different instrument conditions for collecting powder diffraction data (top) 1D intensity as function of d-spacing (bottom) q and 2θ showing the strongly variable peak resolution in backscattering. The data emphasises that refinements in 2D are highly beneficial to take advantage of the higher resolution in the backscattering detectors.

Small angle scattering and multiple length scale instruments:

In general SANS instruments will hugely benefit from the long pulse as most experiments can cope with a low resolution of Δλ/λ = 10%, thereby giving access to a broad wavelength band for a short instrument. HEIMDAL will have a resolution of Δλ/λ = 1.5% at 4.5Å, therefore resolution wise the SANS performance of HEIMDAL will be comparable to the best SANS instruments at sources such as ILL. With regards to the SANS instruments at ESS the length of HEIMDAL does reduce the usable bandwidth. However, the diffraction detectors increase the q-coverage thus the combined small angle and diffraction detectors cover a very

broad q-range using a single pulse. The short band width has the virtue of making the data corrections for absorption and gravity easier as the data is essentially monochromatic. The mentioned benefit comes at the price of reduced flux compared to instruments like ODIN.

Only a few instruments have the capability to cover multiple length scales. However all existing instruments are focused primarily towards one technique with some capability of measuring non-ideal data for the other technique. The instruments in questions for SANS/NPD are D16@ILL, NIMROD@ISIS and three instruments at J-Parc, HI-SANS, Nova and i-Materia. HEIMDAL will outperform the combined instruments at the other facilities, as HEIMDAL is an uncompromised thermal powder diffractometer *and* a high resolution SANS instrument with performance similar to the best SANS instrument at conventional facilities. At present due to lacking data, it has not been possible to benchmark the instrument against instruments such as NIMROD or SANS2d at ISIS, or D33@ILL, nor the ESS instruments LOKE. An overview of *in situ* powder diffraction instruments and broad length scale instrument is provided in appendix B.

1.1.7 Infrastructure and supporting facilities:

HEIMDAL will need a broad sample environment, as the experiments are considered to be *in situ* or *in operandi.* Therefore a large variation in samples shape and sample environment is expected for the instrument. It is foreseen that the instrument should have a sample environment built-up station, comparable to the real instrument, so that users can setup and test their sample environment off-line before the experiment starts. The test station must include all electrical, gas, and water cooling connections. This will ensure that a minimum of neutrons are lost due to changing experimental conditions. The setup also allows for extended time experiments were a sample can be kept at specific conditions for long time periods, but only need neutron investigate for short times periodically. Chemical preparation laboratories should also be present to prepare samples for experiments on-site. The foreseen detector gap at low angles on one side of the instrument will allow easy-access to the sample space and allow for example investigations using pump/probes techniques such as, IR, Raman, UV-VIS. In addition a gas mixing system combined with mass spectrometry and gas chromatography should be available (see appendix C for more information about combined techniques and sample environment).

1.1.8 Software:

The diffraction data collected by HEIMDAL is a map of momentum transfer q and time. Data will be collected in event mode, so the arrival time and q of each neutron will be recorded. Time-of-flight diffraction data is conventionally summed to remove the angular dependency. However, for HEIMDAL and other time-of-flight diffractometers with high angular coverage it will be advantages to analyse the data in two dimensions to benefit from higher resolution at higher angles and longer wavelengths. For this purpose new software has to be developed, which can handle two dimensional data. It may still be necessary to do some time and q-space binning to have sufficient count rates for Poisson statistics. This software would be beneficial for all powder instruments capable of collecting 2D data. It is naturally also possible to sum the data and produce conventional 1D patterns as is conventional at time-of-flight diffractometeres today. In addition new software must be developed for handling refinements of multiple length scale data. For the development of this software we anticipate working in **close collaboration with the Data Management and Software Center at ESS Copenhagen (DMSC)**.

1.2 Description of Instrument Concept and Performance [10 pages]

The instrument description is divided into two parts: The first part gives an overall introduction to the instrument, followed by a detailed description of the necessary components.

Introduction: HEIMDAL is designed as a narrow band thermal neutron powder diffractometer. The narrow band optimally utilizes the brightness of the thermal moderator, see Figure 4. The wavelength resolution is given by $\Delta\lambda/\lambda=\tau/(\alpha L\lambda)$ and it is in other words, proportional to the pulse duration (τ) and inverse proportional to the instrument length (L) and wavelength (λ), while α=252.8 µs/Åm is a constant. The ESS pulse duration of τ=2.86 ms is too long for producing high resolution for short wavelength neutrons (λ<1.5 Å). Figure 5 shows the resolution $\Delta d/d$ as function of wavelength for different instrument length and pulse duration for the backscattering detectors. An instrument designed for crystallographic structural studies needs relatively short wavelength neutrons < 4Å. Consider the standard of $Na_2Ca_3Al_2F_{14}$ ($I2_13$, a = 10.257 Å), with detector coverage 10-160° the number of collectable structure factors dependent on wavelength $\#F_{hkl}@\lambda$, giving: 3560@0.6Å, 250@1.5Å, 77@2.3Å and 16@4.0Å. Even though the 4.0Å neutron will inherently have a good resolution the amount of crystallographic information obtainable is limited.

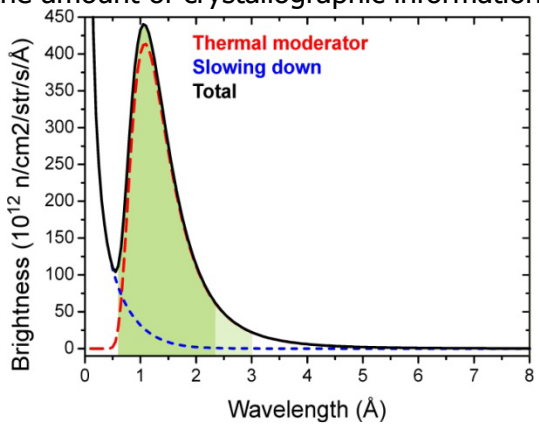

Figure 4 The brightness of the thermal moderator source [P. Willendrup 2014], including the slowed down neutron, spectrum. The green area is reflecting the wavelength range used for the optimization.

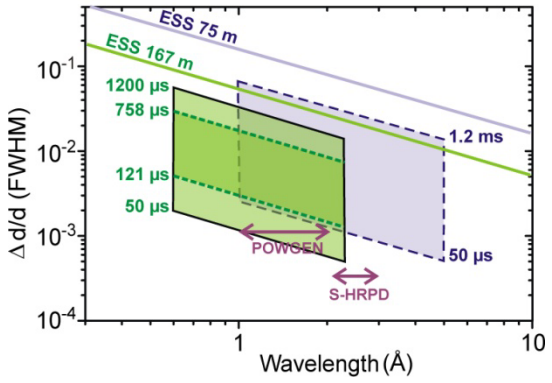

Figure 5 Wavelength range and resolution, green area is for HEIMDAL, while the blue area is equivalent of a 75 m instrument at ESS.

The natural instrument length is L=169 m given by the ratio between the source repetition rate (T=71.4 ms) and the pulse duration (τ=2.86 ms), and position of the pulse shaping chopper (L_{ps} = 6.5 m): $T/\tau=(L-L_{ps})/L_{ps}$. Knowing the instrument length the wavelength band can be calculated: $\Delta\lambda=\alpha(L-L_{ps})/T$ = 1.7 Å. We decide to focus on a optimizing guide performance for neutrons from 0.6-3 Å, with a typical wavelength band of 0.6-2.3 Å, with a mean wavelength of about λ_{mean} = 1.5 Å.

Even at this length the instrument will not provide sufficient resolution for utilizing the full pulse for powder diffraction. To obtain a better resolution a pulse shaping chopper placed close to the monolith gives control over the pulse width. The pulse shaping chopper can select down a pulse width down to 52 µs of the full pulse using a 16 mm opening. This utilizing <1% of the ESS pulse of 2.86 ms. Extracting 758 µs uses about 25% of the full pulse (see Figure 1) and still gives a reasonable resolution see Figure 5. More detailed

consideration regarding the thermal powder diffractometer is found in appendix D. The instrument represents an optimal designed for moderately large structures with unit cells < 25 Å, i.e. unit cell volumes < 15'000 $Å^3$. The instrument is designed to cover a large q-range from 0.6-21 $Å^{-1}$ using a cylindrical detector arrangement from 10-170°. The detector arrangement is illustrated in Figure 6 and schematically in Figure 16. Detectors are placed above and below the incoming beams to fully cover the backscattering region. Wavelengths < 0.6 Å = λ_{min} are not considered, due to short comings of guide transport, chopper and detector efficiency for short wavelength neutrons.

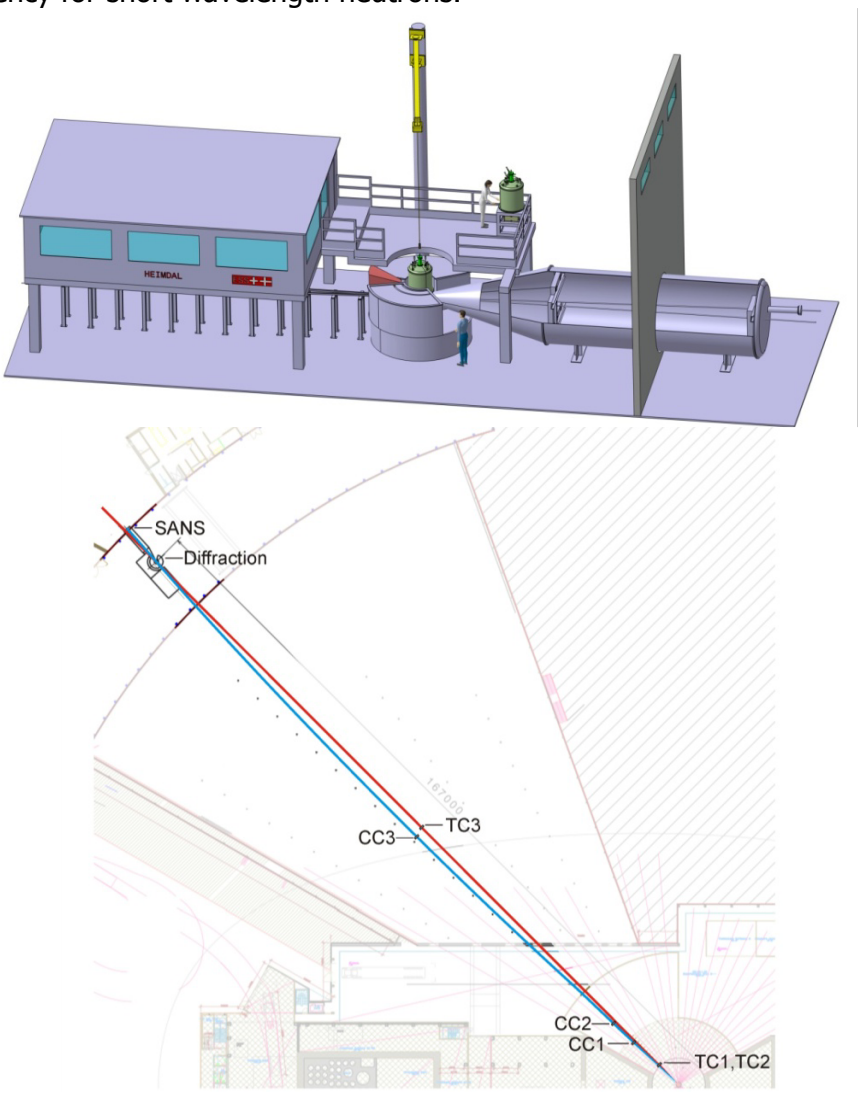

Figure 6 Instrument overview (top) technical drawing of the instrument, from Left to right: Instrument hutch and laboratory area, sample area with access platform for top-loading and off-line testing. At the right hand side wall of ESS hall is shown together with the SANS tank, the tank outside the main ESS hall will be air-conditioned. The backscattering detectors are emphasised by red colouring. (bottom) layout of guide hall and suggested position of HEIMDAL.

In addition to the optimized thermal neutron powder diffractometer (TNPD), the instrument has been designed to accommodate Small Angle Neutron Scattering (SANS) and Neutron Imaging (NI) options. The technical challenges are highly different for the different techniques with respect to resolution and optics: TNDP favors a wavelength resolution ($\Delta\lambda/\lambda$)

< 0.5%, to produces sharp powder diffraction peaks. SANS on the other hand can accept $\Delta\lambda/\lambda$ ~10%, while SANS requires a highly collimated beam. TNPD can increase the flux by focusing the beam through increased beam divergence at the sample position. Finally, a short wavelength is advantageous for TNPD as this allows large coverage of reciprocal space as necessary for PDF. In contrast small angle scattering uses long neutron wavelengths to measure scattering at small q. Therefore **we suggest a novel concept, where two guides - a thermal and a cold guide – is extracted from the same beamport** and transported to the sample position. The thermal guide is optimized for TNPD, while the cold guide is optimized for SANS and partially for NI. The two guides are separated by an angle of 3.5° at the sample position leaving sufficient space for optical components and avoids the thermal beam hitting the SANS detector.

Instrument simulations show the feasibility of extracting two beams from the same beamport and having the beams converging at the samples position at an angle of 3.5°. When operated in hybrid mode, the instrument would allow either a thermal or cold pulses to reach sample. The TNPD and SANS would not operated simultaneous, however the pulse train can be adjusted according to the requirements of the experiment. In other words it is possible to do two TNPD pulses and for every SANS pulse. The situation is illustrated in Figure 7. The SANS will suffer from the long instrument length as the useable bandwidth is reduced. However usage of the diffraction detectors to collect the SANS signal will allow collection of a broad q-range from 0.001-1.3 $Å^{-1}$ using the narrow wavelength band from 9.1-10.8 Å. The reduction of flux scales with the instrument length, however in contrast to TNPD, SANS can utilize the full pulse length and the narrow pulse width eases the data analysis with respect to absorption correction, gravity effects and multiple scattering. Our two-guide setup allows leaving the cold beam unperturbed, while chopping the thermal beam for powder diffraction. This would not be possible by using bispectral extraction, through one guide. Furthermore, having two guides allows for a focused beam for NPD, and collimated beam for SANS. **The two guide setup allows the SANS to be considered an add-on to an optimized thermal powder diffractometer.**

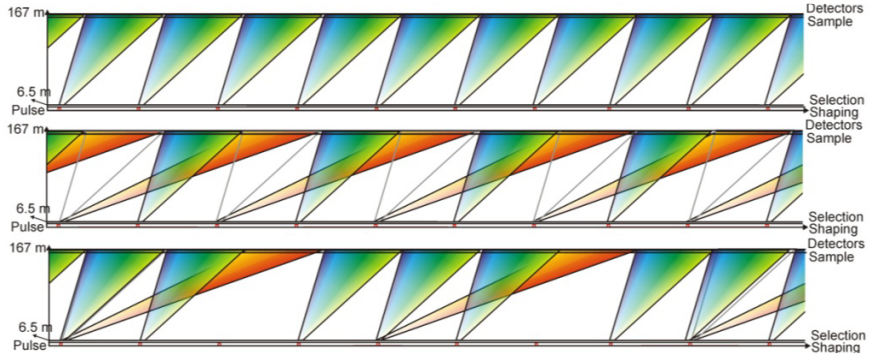

Figure 7 Different pulse trains for cold and thermal neutrons. (top) thermal powder diffraction alone, (middle) equal time for TNPD and SANS, (bottom) 3 thermal pulses for every SANS pulse. The pulse train can adjusted to suppress a maximum of 6 pulses.

The imaging detector is placed as close to the sample as possible and allows real space images of the sample with a resolution down to ~50 µm for samples of <50x50 mm^2. The intention is to use a time resolved imaging detector, which allows Bragg-edge imaging. The Bragg-edge imaging will inherently have sufficient resolution $\Delta\lambda/\lambda$=1.5%@4.5 Å to do phase determination based on the Bragg attenuation of the transmitted beam. However, it cannot be used simultaneously with the SANS detector.

Detailed description of the different components:

The detailed description of invididual HEIMDAL is divided into the thermal guide and the cold guide, while the beam extracting covers both beams.

1.2.1 Beam extraction

The exact positions, shape, and size of the moderators are still under discussion. Consequently, the following description is based on the TDR and discussion with Phil Bentley. At ESS, the center of the cold and thermal moderators will be separated horizontally by a distance of 16 cm. The two beams must go through different openings as only the thermal beam for the TNPD should see the pulse shaping chopper, placed after the biological shielding. The plug dimensions 2 m from the moderator are restricted to 90×200 mm^2 and allow the two beams to be displaced vertically, toward the end of the biological shielding. In case of a pancake moderator, the two beams will be tilted slightly horizontally to avoid collisions. Figure 9 illustrates the geometry and proves the absence of guide collisions. Assuming conservatively that the outer guide dimensions in each direction are 10 mm larger than the inner dimensions due to substrate and support. In total, this leaves up to 20 mm margin between the two guides at the chopper position.

The thermal guide is passed through the plug by a feeder starting at dimensions of 40x80 mm^2 at a distance 2 m from the moderator surface and shrinking to 30×60 mm^2 at the end of the monolith 6 m from the moderator. The pulse shaping chopper is placed 6.5 m from the moderator surface, see Figure 8. The spacing of the cold and thermal guide is illustrated in Figure 8. At the monolith surface the cold guide passes below the thermal chopper system before meeting the first cold chopper CC1 at 14 m from the monolith surface.

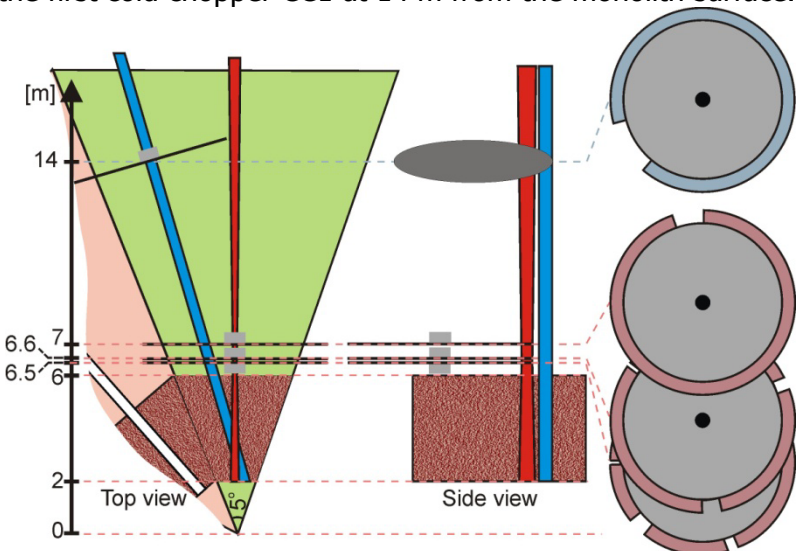

Figure 8: Beam extraction from the monolith, top and side view including chopper arrangement. The thermal beam is controlled through the first choppers, TC1 counter rotating double chopper, TC2 pulse selection chopper. The first cold chopper at 14 m is also shown CC1.

The cold guide is extracted through a 60 x 60 mm^2 guide below the thermal guide, see Figure 9. The beam extraction solution introduces an initial angular deviation between the two guides of 1.8°, the guides must be brought together at the sample position with a separation of about 3.5°.

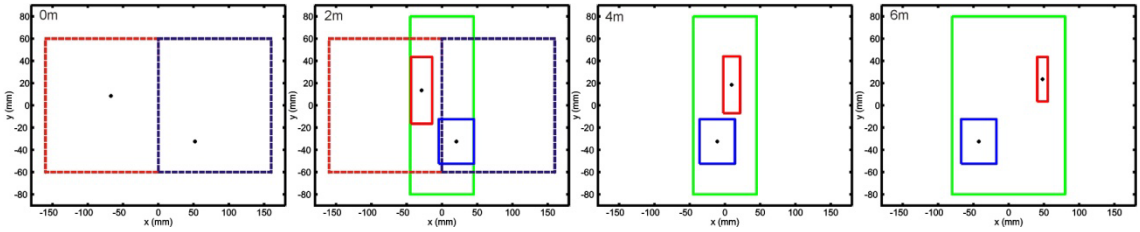

Figure 9: The beam extraction from the cold (blue) and thermal (red) moderator. The figures are different distances to the moderator, (z = 0, 2, 4 and 6 m, from left to right). The figure illustrates the feasibility of extracting a cold and a thermal beam from the moderator using a single beam port without collision.

Design concept: Thermal neutron powder diffraction:
Feeder size: 2m from moderator: H x V 40x80 mm^2, 6.0 m at monolith surface 30×60 mm^2
Moderator to sample distance: 167 m, wavelength band $\Delta\lambda$=1.7 Å, λ_{min} = 0.6 Å
Chopper system: Pulse shaping: 6.5 m, pulse selection: 7m, Frame overlap: 79 m
Beam divergence: Horizontal x vertical: (H_{FWHM} x V_{FWHM}) = (0.5°, 2.0°)
Sample size: Horizontal x vertical 5 x 15 mm^2,
Guide coating: m = 5 (this can be reduced at the straight parts)
Slits: Jaw slits, 4 slits placed in the last part of the guide to control divergence
Sample area: 1 m diameter, top access, plus optical side access.
Radial collimation: 1 m from the sample, exchangeable for different angular openings.
Detectors: Sample distance 1.5 m, cylindrical coverage from 10-170°, pixel size 3 x 10 mm^2

1.2.2 Thermal chopper system:

The thermal guide will have three thermal choppers (TC). TC1 pulse shaping chopper, TC2 pulse selection chopper, and TC3 frame overlap chopper. The pulse shaping chopper and pulse selection chopper are shown in Figure 8.

TC1 - Pulse shaping chopper: The pulse shaping chopper is a fast counter rotating double chopper, first disc is placed 6.5 m from the moderator, while the second disc is at 6.6 m. The pulse shaping chopper runs at 280 Hz, which is below the limit of today's choppers of f_{max} = 350 Hz. However, Iain Sutton pointed out that choppers placed 6.5 m needs to be highly reliable due to close proximity to the source. Three different openings in the pulse shaping chopper are foreseen to allow variations in opening times (dt) from 52-1140 µs. Optimal matching of time and divergence resolution is possible between 121 to 758 µs, resulting in an instrumental resolution of $\Delta d/d$(FWHM) = 0.17-1% for 1.5Å@90°. Best resolution is obtained with 52 µs and 3 Å, where a resolution of 0.03% can be obtained in the backscattering detector (3Å@170°). The disc diameter is 700 mm with the beam position 320 mm from the center of the disc. The pulse length can be increased by spinning the pulse shaping chopper at lower speed. Unwanted neutron passing the pulse shaping chopper are suppressed by placing a slow rotating pulse selection chopper at 7 m (TC2), see Figure 8 for illustration of chopper setup.

TC2 - Pulse selection chopper: Positioned 7 m from the moderator, the pulse selection chopper has two functions: 1) suppressing the long wavelength neutrons allowed by the pulse shaping chopper TC1 and 2) pulse suppression of the entire pulse, allowing the pulse from the cold guide to reach the sample. The pulse selection chopper will be rotating at low speed, at most identical with the source frequency of 14 Hz. A disc with a similar diameter to TC1 will be used to allow the entire chopper arrangement to be lifted in an out of the

protected area enabling faster service in case of hardware failure. Using a chopper window of 20° allows a fully open time of 1.3 ms and a partial opening time of 2 ms, sufficient to allow a single thermal pulse and suppressing the longer neutron wavelengths.

Having the first two choppers rather close together and also close to the moderator will produce ”blurry” edges in the wavelength distribution, e.g. from the neutrons emitted in the time-tail of the moderator. We remove these neutrons by a wavelength definition chopper located half way down the instrument TC3. The suppression of long wavelength neutrons are shown in the time distance diagram, see Figure 10.

TC3 - Frame overlap chopper: The frame overlap chopper is placed at the narrow part of the guide system, approximately half way to the sample, around 79 m from the moderator. The frame overlap chopper TC3 will have an opening angle of 175° and be spinning at the source frequency of 14 Hz, this disc can in principle be allowed to have a larger diameter than TC1 and TC2. This chopper system, allows frame overlap when the neutrons from one source pulse reach the pulse-shaping burst from the next pulse, which occurs for neutrons with wavelengths around 45 Å. However, the flux from the thermal source at this wavelength will be low and the d-spacing has to be >65 Å to fulfil Bragg conditions. A summary of the chopper system can be found in Table II.

	Purpose	Position [m]	v [Hz]	Diameter [mm]	Opening time [μs]	Opening Length L_{max} [mm or °]	Pulse length [ms]
TC1	Pulse shaping	6.5	280	700	26-1200	16, 35 and 70 mm	3.57
TC2	Pulse selection	7.0	14	700	-	20°	2.0
TC3	Frame overlap	78.6	14	700	-	175°	-

Table II: Summary of the chopper system need for the thermal and cold guide. The pulse shaping chopper TC1 is most demanding.

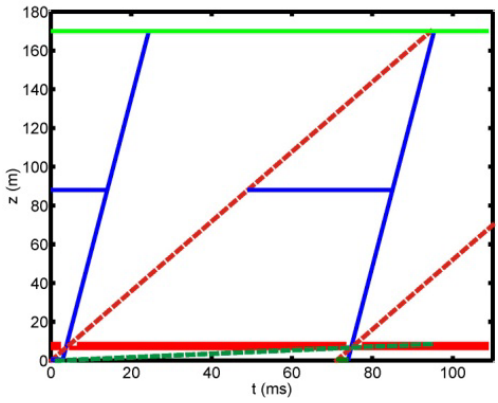

Figure 10 Time-of-flight diagram of a 167 m long diffraction instrument with a pulse shaping chopper at 6.5 m. The neutron position (z) is plotted as a function of flight time (t). Neutrons from two pulses are shown; straight blue lines representing λ = 0.5 Å, dashed red lines representing λ = 2.2 Å., While the green dashed line corresponds to 45Å neutron escaping through the chopper system.

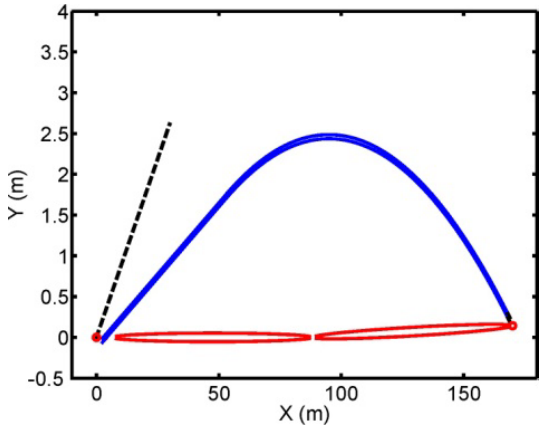

Figure 11 Illustration of spacing of the cold (blue) and thermal (red) guide system when taken from a single beam port. The figure shows enlarged y-axis for clarity. Here, X is the distance from the source. The black dashed line represents the 5° guide segment. The figure is not exactly to scale.

1.2.3 The thermal guide

The thermal guide is designed as a double ellipse separated by a parallel bend section. The setup features once out-of-line-of-sight, see Figure 12. In the simulations m = 5 coatings have been used for all guide sections, however lower m coating values can be used in most of the guide and this has also been considered in cost estimating the guide. We have tested other guide designs including a straight guide with a T_0-chopper, however the once out-of-line-of-sight is the preferred option. The recent development in pancake moderators has also been considered. A brightness gain of about 50% could be obtained by reducing the moderator height to 5-7 cm. Twice out-of-line-of-sight simulations have also been performed for the reduced moderator height, see Appendix E.

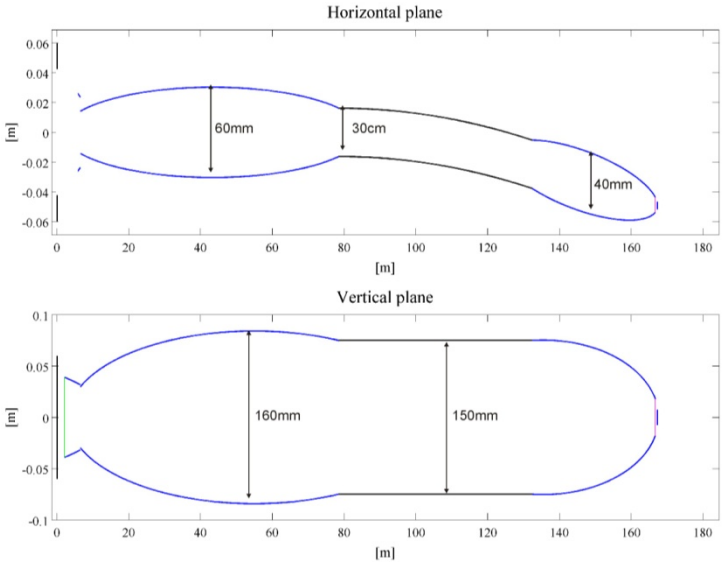

Figure 12: Results from GuideBot optimization. The upper figure is the horizontal plane, while the lower figure represents the vertical plane. The difference in height and width reflects the different divergence requirements.

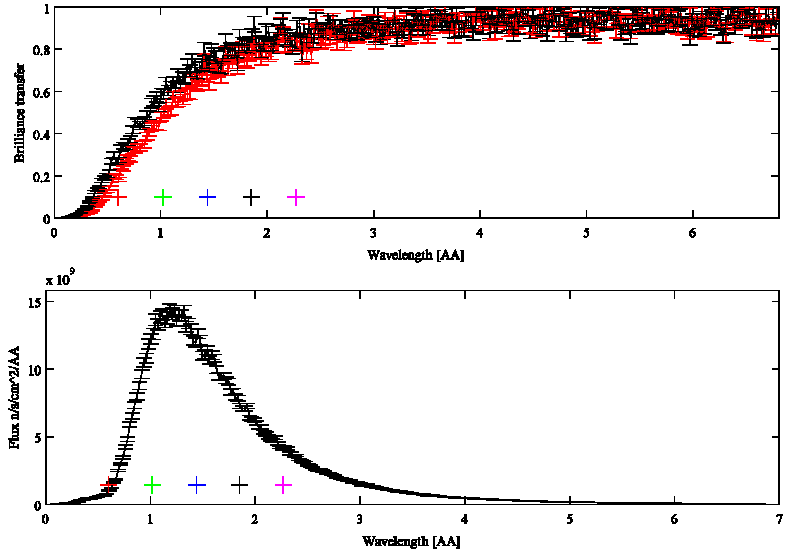

Figure 13: (*top*) McStas simulations of the brilliance transfer (defined as neutron intensity within a certain wavelength, position, and divergence interval). (*bottom*) Time averaged flux of full pulse at sample position: divergence H_{FWHM} = 0.5° and V_{FWHM} = 2.0°.

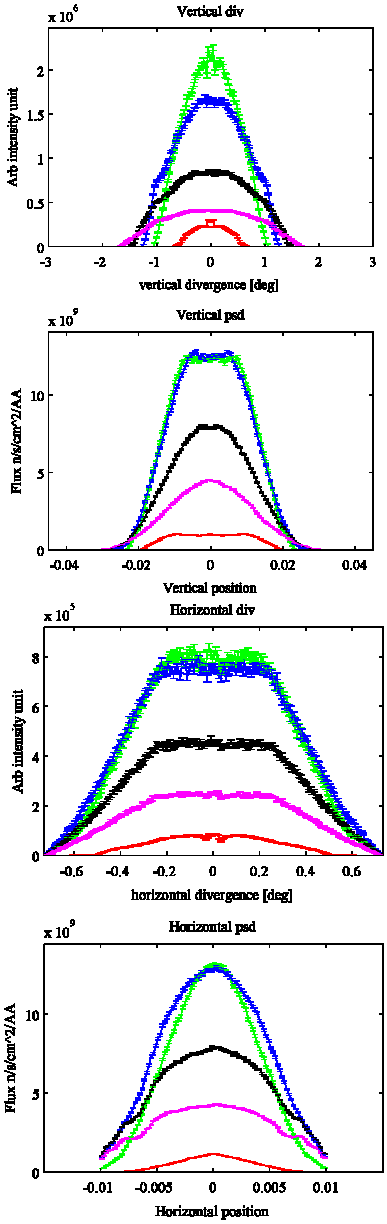

Figure 14: Flux as function of divergence and position. The colors represent different wavelengths red, green, blue, black, purple equal: 0.6, 1.2, 1.5, 1.9, 2.3Å.

The optimal sample size was chosen to be width x height = 5x15 mm^2 matching the detector pixel resolution of 3x10 mm^2. The horizontal and vertical beam divergences are uncoupled and can be controlled individually to H_{FWHM} = 0.5° and V_{FWHM} = 2.0°. A jaw slit system in front of the samples as realized on WISH@ISIS allows control of the divergence to match the beam divergence to the time resolution. An approximation to the beam delivery system is obtained by running the GuideBot software written by Mads Bertelsen[44]. The result from GuideBot is shown in Figure 13. The guide is optimized for maximum brilliance transfer for neutron with wavelength from 0.6-3Å.

The long guide has difficulty in transporting the shortest wavelength neutrons. The brilliance transfer is about 85% for neutron λ > 2Å, while it drops to about 75% for $\lambda\sim$ 1.5 Å and decreases to below 60% for λ < 1 Å neutrons. The sample flux is obtained from the brilliance transfer and the source brightness. The position and divergence dependence of the brilliance transfer is shown in Figure 14. Integrating the time averaged flux curve over the wavelength interval of 0.6-2.3Å gives a time averaged flux of $\sim 2.1 \cdot 10^{10}$ n/s/cm^2. The time averaged flux will be reduced when running the pulse shaping chopper, therefore at $\Delta d/d$@90° = 1% the time averaged flux will be around $2.0 \cdot 10^9$ n/s/cm^2. Increasing the resolution by decreasing the divergence and the pulse length will further reduce the time averaged flux at the sample position.

Thermal guide optics: At the end of the second guide ellipse, an aperture system consisting of four individual apertures controls the beam size as well as the beam divergence at the sample position as on WISH@ISIS. The last aperture before hitting the sample is placed 1.5 m from the samples position, just before the beam enters the detector area. The beam will travel in an evacuated beam tube until shortly before the sample. Depending on sample environment, it is foreseen that the vacuum window will be placed 150 mm from the sample position. The window should be made from single crystal material sapphire or diamond to avoid small angle scattering, which could produce unwanted background for the SANS setup.

1.2.4 Powder diffraction detectors

The powder diffraction detectors are arranged cylindrically around the sample and one side, the detector covers from 10-170° (left hand side) In addition backscattering detectors ensures large coverage of the highest possible angles, giving better statistics for the high Q-values. The dedicated backscattering detectors covers an angular range from 154-172° above and below. During construction the initial detector coverage will be one side fully covered ~4m^2 plus the backscattering detector 0.5 m^2 and from 170-150° on the right hand side adding another 0.5 m^2. During the upgrade the right hand side of the instrument will be covered from 150-55°, this will leave sample access from the side usable for optical access and ease cabling to the sample environment. The detectors are placed at a distance of 1.5 m from the sample position and with a height of 1 m they allow coverage of ±18° in the horizontal plane. We intend to start with close to 5 m^2 on day-1, which is equivalent to detector coverage of 2.25 sr. In the final state the diffraction detectors will have coverage of ~3.25 sr. The limited vertical coverage allows using a highly vertical divergent beam to increase flux at sample position with acceptable lose of vertical resolution. The pixel resolution is (width x height) equal to 3 x 10 mm^2 to match sample size, which is optimized for 5 x 15 mm^2. Scintillation detectors[45] are the most straightforward solution for our needs. Replacing photomultipliers by avalanche-photo-diodes (APD's) such as developed by PSI for the new POLDI detectors at PSI can further improve such detectors, making the primary electronics less sensitive to stray fields from magnets. PSI has recently entered into an

agreement with ISIS for a collaborative effort on scintillation detectors under the EU Horizon 2020 program.

The cylindrical arrangement of the detector ensures a smoothly varying peak profile function both in angular and time space. Together with the almost triangular pulse shape the description of the profile function will be limited to a few parameters. This ensures easier data treatment compared with conventional spallation sources, where each detector bank in some cases is treated independently. A simulated data set of is $Na_2Al_{12}Ca_3F_{14}$ is shown in Figure 15.

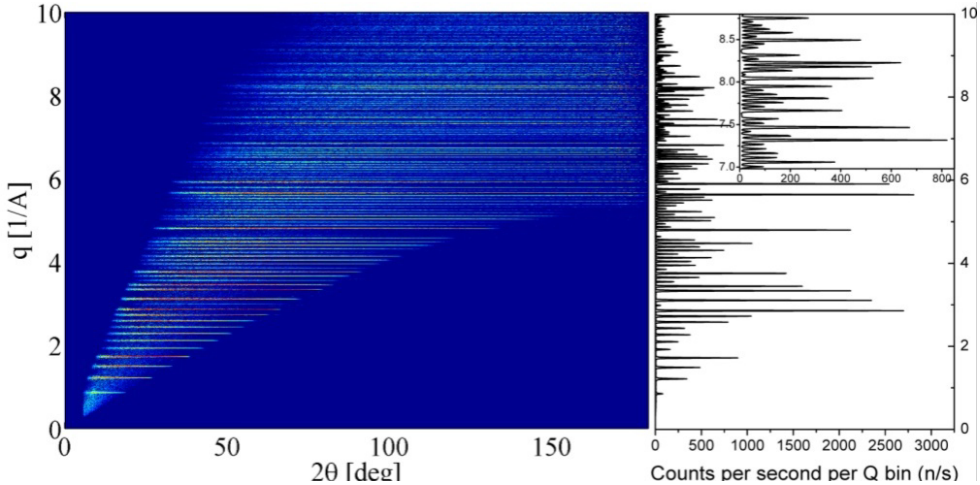

Figure 15: (*left*) Simulation of the powder diffraction pattern for HEIMDAL with the instrumental design described below. The pulse width is 121 µs, while the horizontal and vertical divergence is H_{FWHM} = 0.1° and V_{FWHM} = 0.5°. The sample is $Na_2Al_{12}Ca_3F_{14}$. (*right*) The summation of the 2D plot gives an idea about the intensity and resolution. The insert shows a range around 8.2-9 $Å^{-1}$.

The cylindrical arrangement allows 2D refinements of the diffraction data as described in 1.1.8 software development for ESS. Figure 16 shows the instrument overview including the different detectors.

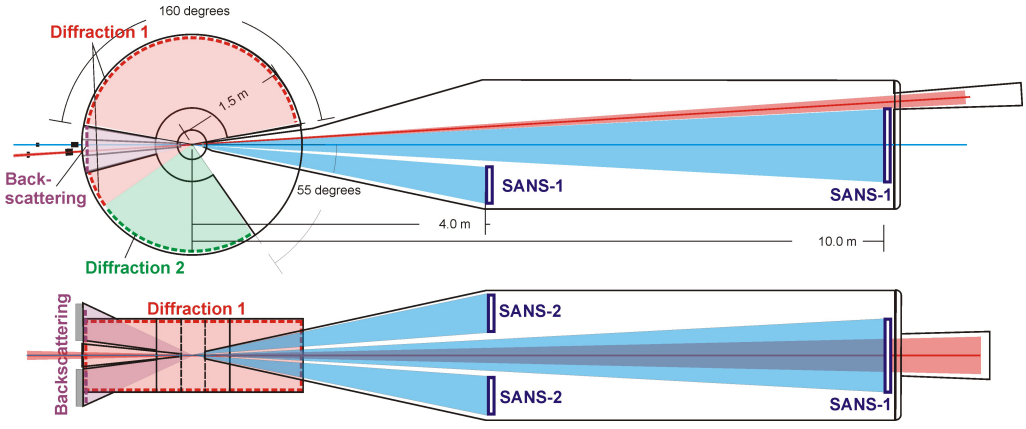

Figure 16: Detector setup (top) view from above, (bottom) side view. The backscattering detectors are above and below the incoming beams as seen below. The SANS detectors at 4 m above and below the horizontal plane is not shown in the top view, while the side detector is not shown in side view. The NI detector and the radial collimator are not shown.

1.2.5 Radial collimation:

The volume between the sample and the detector from 0.5 to 1.5 m will be filled with Ar or dry air to avoid scattering from moisture in the air. In the standard configuration a radial

collimator: 600 mm high and 300 mm wide, with a blade separation of 1° will be installed 0.5 m from the sample. It should be possible to automatically lower the radial collimator out of diffracted beam. This possibility gives an option for easily changing to another collimation system to fit the sample size and the sample environment. Ideally, it should be possible to build the collimators into the sample environment and make it easily interchangeable. The immediate volume around the sample and sample environment will be evacuated. A vanadium window will seal between the prevacuum around the sample and the Ar in the diffraction detector tank. The sample vessel should be removable for specialized sample environment and allow space of up to 1 m diameter. Normally the sample and sample environment will be top loaded and rubber seals will be used for the evacuation.

1.2.6 The sample environment

The success of ILL and in the follow up by many other larger scale facilities is the **availability, but also the standardization of the sample environment**. Sample environment should be exchangeable between most instruments, easy to mount, easy to operate and easy to control. As a consequence, the design of the sample position will allow most standard sample environment as for example used by POWGEN@SNS, D20@ILL, SPODI@FRM2 or HRPT@SINQ. The sample table height should be selected to be something like 500 mm below the beam center (ESS management is expected to standardize this for all instruments). The space should be sufficient for built-in crossed translation tables (correction of small sample misalignments).

Automatic sample changers allows a high through-put of experiments in the standard temperature range from 2 to 350 K and should be considered as mail-in service may become an option for user access. Sample spinning or oscillation will be possible to ensure random orientation of crystal grains with respect to the incoming beam. Special care will be taken to optimize the physical access to the sample area and the auxiliary installed by building a platform above the instrument area. Our targets in the main fields regarding sample environments are shown in Figure 17:

- Temperatures between 10 mK and 2000 K
- Automatic sample changer in the temperature range 1.8-350 K
- Vertical magnetic fields up to 15 Tesla at temperatures 1.8-300K, special cases 50 mK
- Uniaxial pressure up to 20 GPa at temperatures down to 3 K
- Electric fields up to 10 kV/mm at temperatures down to 1.8 K

Figure 17 From left to right: multi low temperature sample changer, orange cryostate, closed cycle cryostate, cryomagnet, pressure cell, high temperature furnace. (Pictures PSI, ILL, FRM2).

In addition to standard sample environments, we expect that the drive for *in situ* or *in operandi* studies **requires special and flexible sample environment** as users will come from different scientific areas bringing their own equipment. The incident optical components and radial collimation should be easily interchangeable and this is likewise true for vacuum windows in the sample environment. The sample space should be easily accessible from the

top and from 35° on the right hand side. The side access gives optical access to the sample for irradiation by UV-VIS or IR, including Raman and other optical characterisation methods.

Space will be allocated to setup the next sample environment close to the instrument, including control through the instrument software. Special care has to be taken for controlling and monitor the sample environment, both, on-line and off-line. It is important, that the software control allows parallel operations of different sample environment: The running experiment and the standby experiment. The pretested sample environment should be easily transferable to the beam position. This minimizes the dead time between experiments. It is envisaged, that the complete sample environment can be tested off-line including all cables connections. As the previous beamtime ends the entire sample environment can be pulled out of the instrument and the next sample environment can be inserted with a minimum of setup time, yielding the highest possible reliability during experiments. In this fashion, long term experiments can be inserted at various times (day, weeks, months) without removing the sample from the sample environment. See appendix C for more consideration on the sample environment.

A gas rig for purging different inert and reactive gasses over the sample is foreseen to be available along with gas analysis techniques such as mass spectrometry and gas chromatography. Thermogravimetry (TG) and differential calorimetric scanning (DSC) can also be combined with neutron scattering.

In summary, it is highly important to allow remote changes of temperature, pressure, electric and magnetic field. We will take special care to this point and allocate a limited amount of money in our instrument budget to cover some basic sample environment. We do not see this in contradiction to previous statements (completely exchangeable sample environment between the instruments), as using the same pool and same standard in the sample environment must be a baseline at ESS for well maintained and well calibrated instrumentation and can reduce the operating costs of the instruments drastically, as less personal as well as less backup auxiliary instrumentation will be necessary.

Summary: Cold guide:
Feeder and guide size: 60x60 mm^2
Moderator to sample distance: 167 m, fixed by thermal guide
Chopper system: Band definition chopper 14 m, 2 frame overlap choppers at 18 and 78 m
Guide coating: m = 2
Slits: Double pinhole collimation for SANS 10 m from sample, Single pinhole for NI
Detectors SANS: Flat panel detectors placed at 10 m and 4 m, pixel size 4x4 mm^2
Detectors NI: Timepix: resolution 50 x 50 µm max size 50 x 50 mm^2.

1.2.7 Cold chopper system:

Cold guide chopper system: The resolution $\Delta\lambda/\lambda$ for a full pulse at λ=4.5 Å is $\Delta\lambda/\lambda$ = 1.5%, which is better than normally needed for SANS and therefore, no pulse shaping chopper is necessary. Three slow revolving disc choppers are needed: CC1) wavelength band definition chopper, CC2) frame overlap chopper, CC3) frame overlap chopper. Velocity selectors that often are used at continuous sources are not beneficial as the length gives the natural high resolution and the limited wavelength band.

CC1) *Wavelength band definition chopper*: This chopper must be placed within the first half of the instrument length and as close to the moderator as possible. To avoid interference with the choppers in the thermal guide, we chose to place this wavelength band definition

chopper 14 m away from the moderator in the straight section of the guide. The chopper will spin at source frequency (14 Hz) and have a disk diameter of 700 mm. The chopper should allow the full 2.86 ms pulse to reach the sample. At 14 m the pulse width is about ~10 ms with 14 Hz rotation frequency leading to an opening angle of ~50°**.**

CC2) *Frame overlap chopper #1*: Like for the thermal guide a frame overlap chopper will be placed half way between the moderator and the sample. This chopper is also spinning at source frequency and has a diameter of 700 mm. The opening angle of the frame overlap chopper is just below 180°. Frame overlap is found when slow neutrons from one pulse match the burst time of the wavelength definition chopper meant for neutrons from the next pulse. The wavelength in the wrong frame is 25 Å higher than that of the first frame. Therefore a third chopper is placed at 18 m from the source.

CC3) *Frame overlap chopper #2*: This chopper is placed 18 m from the source and will prevent the neutrons with wavelength +25 Å to pass through the previously described system. A summary of all the chopper system is found in Table III.

	Purpose	Guide	Position [m]	v [Hz]	Diameter [mm	Opening time [μs]	Opening Length L_{max} [mm or °]	Pulse length [ms]
CC1	Band definition	cold	14	14	700	-	50°	10
CC2	Frame overlap	cold	78	14	700	-	175°	-
CC3	Frame overlap	cold	18	14	700	-	175°	-

Table III: Summary of the chopper system need for the cold guide.

1.2.8 The cold guide

Due to the difficulty of transporting thermal neutrons and the wish for having an optimized thermal powder diffractometer the angular separation of the two guides by 3.5° is obtained though curving the cold guide. An 8 m straight guide with dimensions of 60x60 mm^2 is placed 2 m from the moderator below the thermal guide. The beam extraction introduces an initial angular offset of 1.8° between the two guides. After the initial straight section, the cold guide curves 0.5° to quickly get out of line-of-sight, this is followed by another straight section. After 24 m, we have a 125 m long curved guide that bends the beam by an angle of 5.5° to reach the sample with an angle of 3.5° with respect to the thermal beam. The resulting curvature is 1.2 km.

The curved section is approximated by piecewise linear guide pieces. This produces an intrinsic loss of intensity due to small, repeated misplacements from the optimal shape. We have illustrated the effect by carrying out simulations with both 20 and 5 cm pieces of guide. Consequently, for 5 cm pieces the transmission of 5 Å neutrons is 90% for perfect reflecting m=2 mirrors, and 85% for a more realistic reflectivity value of 99.5%. Approximating the curved guide by 20 cm guide pieces gives a considerably worse transmission. Guide loss effects become stronger for narrower guides, due to a larger number of reflections. The wavelength dependence on the guide transmission is shown in Figure 18. The brilliance transfer for neutrons > 6Å reaches almost 100% using 5 cm pieces and only 75% when using 20 cm guide pieces. The divergence profile has not yet been finally analyzed.

Cold guide optics: The SANS setup is envisioned with a double pinhole collimation and a collimation length of ~10 m – identical to the sample to detector distance. By removing the front aperture, a single pinhole camera can be made with a L/D ~ 350 using a 20 mm aperture. A horizontal and vertical divergence of $H_{FWHM} = V_{FWHM} = 0.5°$ gives an illuminated area of with radius of approximately 60 mm. The beam divergence could be reduced by using an aperture closer to the sample.

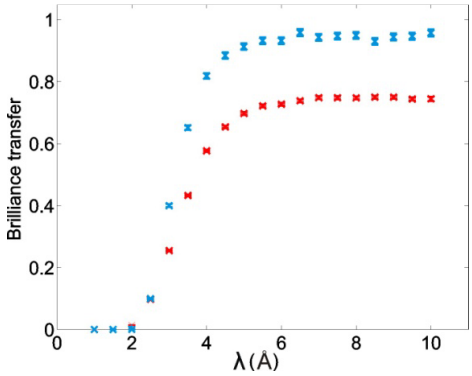

Figure 18 Brilliance transfer of the cold guide shown as a function of the wavelength, λ for two m=2 and two differently sized guide pieces 20 cm (red) and 5 cm (blue).

1.2.9 Small angle scattering detectors

Dedicated small-angle scattering detectors collect the cold neutrons together with the diffraction detectors. The dedicated small angle scattering detectors are placed in two different positions: 1) A flat panel detector placed 10 m from the sample with a size of 1x1 m^2 and a pixel resolution of 4x4 mm^2, 2) three half sized flat panel detectors (1x0.5 m^2) placed 4 m from the sample displaced away from the central beam as seen in Figure 16. The fourth detector is missing and allows a get lost beam tube geometry for the thermal beam. The diffraction detectors are used to extend the q-range of the small angle scattering setup. Flat panel detector will be based on present ESS developments with state-of-the-art ^{10}B technology, or ^{3}He depending on the development of the ^{3}He availability.

When including the NPD detectors for collecting the SANS signal a very broad range can be covered in a single setting. The detector coverage as function of wavelength is illustrated in Figure 19. A 3 cm diameter beamstop placed 20 cm from the detector surface, results in a possible coverage of $q=4\pi\sin\theta/\lambda$ from q_{min}(11 Å, SANS)=0.001 $Å^{-1}$ to q_{max}(4 Å, NPD),=3 $Å^{-1}$. Using only a single pulse in the wavelength range 9.1-10.8 Å gives full coverage in the region 0.001-1.3 $Å^{-1}$. A calculation of the detector coverage using 9.1-10.8 Å is shown in Figure 20. The scattering curves are calculated for hard spheres with diameters of 2 nm and 100 nm and with an assumed polydispersivity of 10%.

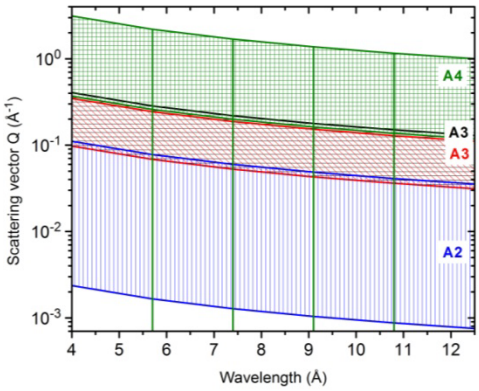

Figure 19 The detector coverage for the cold guide depending on wavelength and detector. The red dashed line show the limit of full coverage or pseudo full coverage, due to the square shape of the detector.

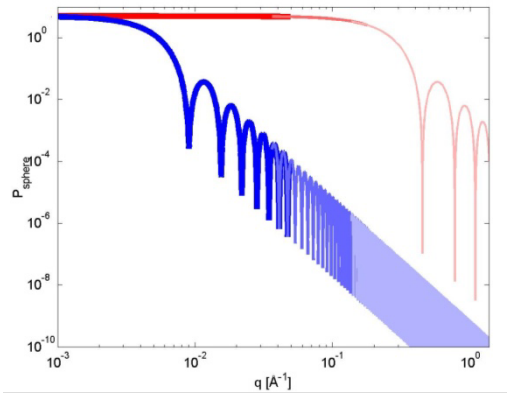

Figure 20: Calculation of two spherical particles of diameter 2 nm (red) and 100 nm (blue) using the wavelength range from 9.1-10.8 Å. The different line widths represent different detectors.

Based on the above calculations a single narrow wavelength band is sufficient for collection of SANS data. If necessary a wider wavelength band is possible through pulse suppression. Pulse suppression is also used to separate the individual pulses from powder and small angle scattering. In other words the time window on the detector will be dedicated to either small angle scattering or powder diffraction.

1.2.10 The sample geometry considerations:

Conventionally different sample geometries are used for NPD and SANS. Typical for NPD is a cylindrical geometry giving uniform scattering in all directions, while SANS uses thin flat sample geometry to have an even attenuation across the entire surface of the sample. In our simulations, we are optimizing for a cylindrical sample with dimensions of 5 mm diameter and 15 mm of height. When working with non-hydrogenous samples in SANS it is not necessary to work with thin samples and the variation in thickness across a cylindrical sample can relatively easy be corrected. Especially when using an almost monochromatic beam as is the case for the narrow bandwidth of HEIMDAL. Flat samples as traditionally used by SANS are naturally also usable, but the detector coverage (diffraction detectors) is likely limited to 45° or less due to angular variation in attenuation. Flat samples would not be good for the 90° detector banks, but we are expecting to be able to cope with complicated sample shapes and sample environment. We intended that the data reduction software should be capable of dealing with different sample geometries and attenuation corrections.

1.2.11 Imaging station

The imaging option is operated as an add-on unit, which can be activated on demand, but not operated in sequence with the 14 Hz ESS pulse frequency. The imaging camera will be placed within the sample chamber normally kept under vacuum. For the operation of the SANS option, the camera has to be moved completely out of the beam area. This can be solved by approaching a parking position, which is beyond the beam, but still within the vacuum chamber. In the operating position, the camera should be placed as close as possible to the sample to avoid loss of resolution. The design will allow both neutron beams (thermal and cold) to be used for imaging, even with the 3.5° offset of the two beams. Possible detectors are the Timepix/Medipix[47] detector or a small imaging detector built at PSI (using a CCD camera viewing a scintillation plate over an optical mirror). The two different setups are shown in Figure 21. The Timepix/Medipix detector has two main advantages: 1) it allows time resolved Bragg edge imaging and 2) it can be placed much closer to sample, due to the absence of spacious mirror setups, which allows higher resolution. The intended resolution is ~50 µm for samples up to 50x50 mm^2. The Bragg-edge imaging will inherently have sufficient wavelength resolution $\Delta\lambda/\lambda$=1.5% at 4.5 Å due to the length of the instrument. The limitation of the present Timepix/Medipix detector is the low active area size (2.8x2.8 cm^2), which needs limited R&D to be extended to 50x50 mm^2.

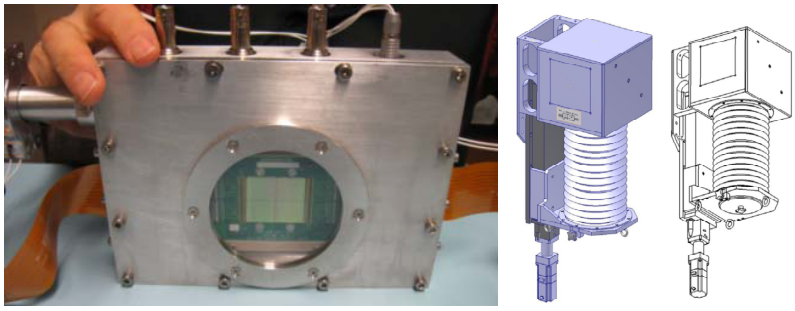

Figure 21 (*left*) the medipix detector with an active area of 28x28 mm^2 and a sampling rate of about 1200 Hz. (*right*) classical imaging setup made with fluorescent screen mirror and CCD.

1.2.12 Summary of the HEIMDAL detectors

The list in Table IV summarizes the detector specifications of HEIMDAL.

	pieces	Size horizontal, vertical [cm]	Total area [m^2]	Pixel reso-lution [mm]	Max. overall count rate ($c/s/cm^2$)	Max. count rate on spot, spot size ($c/s/cm^2$)	Efficiency
NPD	1 2	100x450 100x250 &)	4.5 2.5	3x10	10^4	10^5	50%@1Å 70%@5Å 100%@10Å
NPD Back-scattering	2	50x50	0.5	3x3	10^4	10^5	50%@1Å 70%@5Å 100%@10Å
SANS	1 1 2	100x100 50x100 50x100 &)	1 0.5 1	4x4	10^4	10^4	75%@5Å
NI	1	3x5 (2.8x2.8)	.002	0.05x 0.05	Not critical	Not critical	Not critical

Table IV: Summary of the detector specifications of HEIMDAL &) upgrades

The concept of the multiple-length scale instrument HEIMDAL is based on existing instrument concepts for powder diffraction, small angle scattering and imaging. The challenge is merging these concepts into a single instrument.

1.3 Costing and maturity[2 pages]

This section has been divided into two parts, covering cost and maturity. The page limitation is exceeded considerably, but this was sanctioned at the STAP meeting in December 2013.

The cost estimates for HEIMDAL can be divided into cost related to the thermal and the cold beam. In general six different components can be identified:

- Neutron guide system
- Choppers including electronics
- Sample surrounding (slits, sample positioning, sample chamber, sample mechanics)
- Detectors (including mechanics, electronics)
- General electronics and computing
- Shielding (primary 5° sector and Instrument)

1.3.1 Neutron guides system

Thermal guide: Length 164 m long with variable, but relative high coating value (m). The thermal guide consists of two double-elliptical sections, eventually with a feeding section. The coating will likely be m=5 in parts of the guide, with a potential to use sections with lower (and consequently less expensive) coating. Our calculations are based on a pseudo-trapezoidal approximation of the elliptical shape. We expect a cost of 2800 kEuro for the thermal guide (excludes 830 kEuro for the mechanical support).

Cold guide: The cold guide is coated fully by m=2 and has a size of 6x6 cm^2. The price is here estimated to 1283 kEuro (includes 417 kEuro for the mechanical support).

1.3.2 Choppers including electronics

Thermal chopper: The main cost is laying in the first pulse shaping chopper with an estimated cost of 350 kEuro, while the other two choppers are estimated to 50 kEuro each. The cost estimates includes the electronics.

Cold chopper: The three cold choppers are all simple choppers with approximate cost of 50 kEuro including control electronics.

1.3.3 Sample surrounding/instrument mechanics

The sample environment contains a vacuum tank, xyz table for the sample positioning, and a positioning system for the imaging camera. All materials chosen for this area must have low magnetic permeability. The costs are expected to be around 520 kEuro. We add 400 kEuro here for sample auxiliary.

1.3.4 Detectors and detector electronics

Diffraction detectors: Detector costs are difficult to estimate as many development projects are ongoing. We are starting with coverage of approximately 4.5 m^2. Based on communication with instrument responsible at ISIS and J-Parc we estimate a cost of 500k€/m^2 giving a cost of 2250 kEuro. Detector mechanics is included in this number. The backscattering detector needs better spatial resolution and we assume a price of 300 kEuro for the 0.5 m^2 needed coverage. Addtionally is mechical supported with an estimated cost of 500 kEuro needed.

SANS detectors: For the SANS detectors, an aluminum vacuum tank of approximately 60 m^3 volume is necessary. Detector electronics inside has to be cooled from the outside. Expected costs are around 300 kEuro for the mechanics only. The total SANS detector coverage by primary detector and secondary detector is 2.5 m^2. Estimated costs are 3750 kEuro

1.3.5 Electronics (motor drives, computing, security system)

Operating this three-in-one instrument will need significantly more electronics compared to a standard single purpose instrument. State-of-the-art electronics will be around 430 kEuro including computers. Electronics also includes the instrument safety system.

1.3.6 Shielding costs

1) Secondary shielding: This includes the remaining guide shielding (164m) and the sample area shielding and will mostly be low cost concrete (1000m^3). Expected costs are 400 kEuro. The thermal guide is in a mostly self-shielding tube included in the price of the guide. Special care and more expensive shielding are needed for the beam-entrance to the sample area (200 kEuro) with materials similar to the primary sector described later in 3) for the 5^o sector closest to the source as well as the sample area (200kEuro).

2) Shielding of the detectors: 500 kEuro will be needed for specialized shielding material, e.g. materials such as borated alu-matrix-materials, and borated plastic materials for shielding against thermal neutrons in the first phase, 200kEuro when completing the PD bank.

3) Shielding primary sector: The 5m thick shielding of the 5 degree sector starts at a radius of 6.5m and ending at 11.5m. It covers 1.5m above and below the beam level. We

need here a composite shielding with high accuracy as many mechanical parts such as chopper, filters, slits are located here and their background has to be eliminated. We are using here the effective costs spent for the EIGER spectrometer built at SINQ to get the costs per volume, as this existing spectrometer is facing a similar radiation spectrum as HEIMDAL at ESS. The volume of this sector for HEIMDAL sums up to 12 m^3 and we expect cost of 1500 kEuro. This seems high, but high precision machining of heavy parts, which involves steps, limiting gaps, access to choppers, etc.). Not only HEIMDAL, but also the neighboring instruments will benefit from a high-quality shielding of this sector, and the cost are therefore taken out of the HEIMDAL budget and listed separately as it may be part of the ESS source.

1.3.7 Manpower

The project needs a post doc. for 3 years/fulltime, 1 year of a senior scientist for supervision, 6 years/50% of a leading scientist for the full period, adding up to 7 person-years or approximately 2240 kEuro based on full-costs basis.

The personals costs of a designer (6 years) as well as 2 technicians (12 years in total) are included in the costs below as the numbers are showing full-costs. Building it internally by a university would reduce the costs accordingly. Upgrading with diffraction detectors are expected to need 1.5 persons for 1 year each.

HEIMDAL Cost and Manpower Estimates	Pcs	Costs/pcs	NPD	SANS	Upgrades
Neutron guides			**4016**	**1283**	
Beam extraction multichannel guide and feeder for the thermal guide	1	300	300		
Thermal elliptic guide, m=max.5, L=164m, coating max m-5, optimized in the center to m=2-3	1	2800	2800		
Thermal guide, mechanical support	1	833	833		
Thermal guide, installation	1	83	83		
Cold Guide, max M=2, M optimized, L=164m	1	808		808	
Cold guide, mechanical support	1	417		417	
Cold guide, installation	1	58		58	
Choppers (details see table II) inclusive electronics			**450**	**150**	
TC1, pulse shaping chopper, f=280Hz, D=700 mm, counter-rotating disks	1	350	350		
TC2, pulse selection chopper, f=14Hz, D=700 mm	1	50	50		
TC3, frame overlap chopper, f=14Hz, D=700 mm	1	50	50		
CC1, band definition chopper, f=14Hz, D=700 mm	1	50		50	
CC2, frame overlap chopper, f=14Hz, D=700 mm	1	50		50	
CC2, frame overlap chopper, f=14Hz, D=700 mm	1	50		50	
Detectors, detector electronics and radial collimators			**3550**	**2640**	**3200**
Cylindrical scintillation detector banks: 1000mm high, R=1500mm, 10-170deg (left), 150-170deg (right) – Diffraction 1 1000mm high, R=1500mm, 55-150deg (right) – Diffraction 2	 4.5 m^2 2.5 m^2	500/m^2	 2350		 1250
Detector mechanics for cylindrical detector banks	2	250	500		
Backscattering detector unit, 2x 0.5m x 0.5m, resolution 5mm	0.5 m^2	600/m^2	300		
Radial collimator, 155 deg. 1000mm high, 1deg resolution	2	300	300		300
Mechanics for oscillating collimator	2	100	100		100
SANS PSD, 1 x (1x1m^2) and 3 x (1x0.5m^2), resolution 4 x 4 mm^2 SANS PSD, 2 x (1x0.5m^2), resolution 4 x 4 mm^2	1.5 1	1500/m^2		2250	 1500
SANS PSD Tank	1	300		300	
SANS nose	1	50		50	
SANS protection booth, 8m long,3m high, 3m wide, air conditioned (outside of conventional building)	1	40		40	
Imaging Option					50

Sample area, sample control area			**520**		
Vacuum box, shielding of sample area	1	200	200		
xy stage for exact sample centering	1	50	50		
Instrument hutch and laboratory space	1	100	100		
Working platform for experiment access	1	50	50		
Slits systems	4	30	120		
Electronics and computing			**430**	**30**	**30**
Instrument control electronic (without choppers and detectors)			400	30	30
Local computing			30		
Dedicated sample auxiliary (not part of ESS pool)			**400**		
Low temperature sample changer	1	200	150		
Robotics for room temperature sample changer	1	50	150		
Gas rig, mass spectrometer, gas chromatography	1	100	100		
Shielding			**1000**	**300**	**200**
Secondary Shielding: Instrument	1	400	400		
Detector shielding	1	700	200	300	200
Secondary Shielding: Guides (thermals guide is mostly self-shielded)	1	400	400		
Shielding primary sector (part of ESS), 5 degrees	1	1500	ESS		

Total HEIMDAL Investments			
Total without standard sample environment	10366	4403	3430
Total man power needed (kEuro)	2240	200	200
Reserve for unforeseen hardware and manpower (10%)	1260	613	213
Total instrument for the different stages	13866	5216	3843
Total instrument primary phase (NPD + SANS)		**19082**	
Total with upgrade			**22925**

ESS Pool Investments:

Standard sample environment (out of ESS pool)			**450**	**50**	
ILL cryostat, 1.5 – 300K	1	80	80		
Cryofurnace, 2-550K	1	120	120		
Vertical magnet, 11T, 4-300K	1	500			
Paris Edinburgh cell, 30 GPa with pressure system	1	100	100		
Dilution insert for ILL cryostat, 20mK	1	150	150		
Gas insertion system for multiple gases	1	70			
Special adaptions for SANS	1	50		50	

Design and Supervision Personal, phase 1	Year 1	Year 2	Year 3	Year 4	Year 5	Year 6	All years
Person months Denmark, Aarhus project group	4	4	2	2	2	2	16
Person months Switzerland, PSI project group	2	2	2	2	2	2	12
Person months leading scientist, ESS	6	12	12	12	12	12	66
Person months leading mechanical engineer, ESS	6	6	24	12	12	4	64
Person months, leading electrical engineer, ESS	4	4	12	4	2	2	28
Person months, computing scientists, ESS	1	1	4	8	12	12	38
Total Manpower in PM	23	29	56	40	42	34	224
Total Manpower in kEuro (1 PM = 10 kEuro)							**2240**

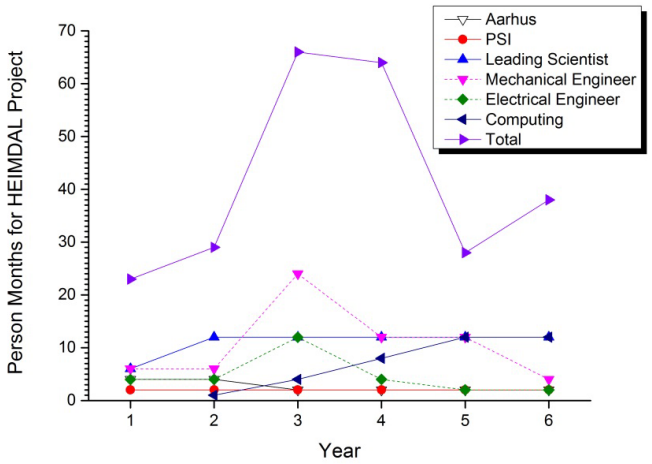

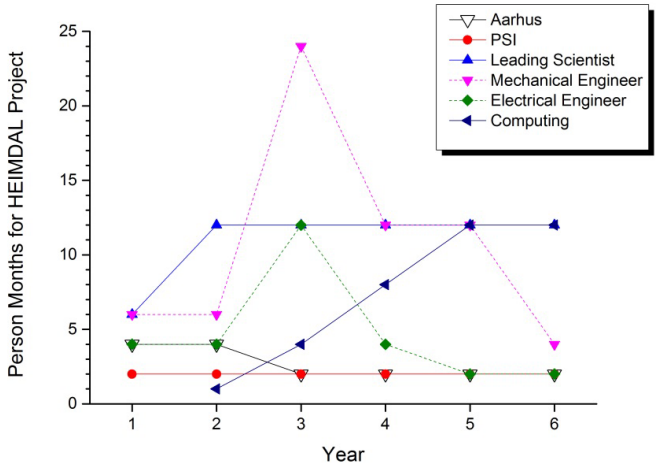

1.3.8 Maturity

The following gives a short overview of the maturity of the individual components, finally a table is giving an overview of risk and possible manufactures for key components.

1.3.9 Guide system:

Using two guides from the same beam port converging at the sample position is a new and challenging concept. The guides can be optimized individually, which is a major advantage to a single guide instrument. The thermal guide for diffraction is challenging (double elliptical double ellipse with high m=5 in some places compared to the m=3 guide for HRPD@ISIS build by SwissNeutronics (SNAG)). The length of curved cold guide is not a standard solution, while the radius of curvature of 1200 mm is quite common. Some development may be necessary to improve the alignment of the individual pieces and thus the transmission. These concepts can be tested on smaller scales *e.g.* using BOA@SINQ.

1.3.10 Chopper systems:

All chopper parameters are all in the range of operating instruments and only space limitations due to the two guides and also neighbouring guides will become a challenge. Having pulse shaping choppers close to the source at ESS will be a general challenge. Forschungszentrum Jülich [FZ] and Astrium are potential industrial partners for the production.

1.3.11 Beamstops:

The two-guide-design needs special attention to stop the beams. Lost-beam-geometry seems to be an appropriate approach, but is challenging as space is limited. A further challenge here is avoiding interference between the thermal beam and the small angle detectors.

1.3.12 Alternative pulse-use for the thermal and cold guide:

This concept needs clear separation of the pulses and taking care of the background from "secondary" sources e.g. the prompt pulse, choppers, slits. A special effort must be placed on the sector from 6.5 m to 11.5 m distance from the source to reduce the background. The calculations for this concept has been successfully applied to the shielding of instruments such as EIGER@SINQ and experimental results have proven it's maturity on a instrument facing a similar neutron spectra as that at ESS.

1.3.13 Detectors:

The availability of huge area detectors may be the most limiting factor for a majority of ESS instruments. The prize can limit the affordable area and as a consequence the performance of the instrument. Stability and background sensitivity (γ-suppression) of the detectors can be a limiting factor for HEIMDAL with its relatively open geometry and unpredictable sample equipment brought-in by the user. However, the detectors have fall-back options using present technologies, but here unpredictable cost can limit this option. PSI is presently building the new POLDI scintillation detector with APD's which could be a basis for the PD detectors of HEIMDAL.

1.3.14 Sample environment:

On one hand, using an evacuated sample area reduces the background, but may limit the user-access with dedicated auxiliary equipment. Special care will be taken here to fulfil different needs: fitting standard pool auxiliary as well equipment brought-in by the user.

1.3.15 Shielding

Shielding especially in the primary sector is demanding. Special care is needed to host and service components such as choppers. Calculating the shielding efficiency is a key issue to minimize the size and optimize the efficiency. The PSI group of U. Filges is highly experienced here to deliver such calculations as proven on the EIGER shielding at SINQ. Also here manufactures for such shielding partially heavy and of high accuracy, could be found (alpha Beton, Hinneburg).

In summary, the maturity of the instrument HEIMDAL is given. All the single components have been realized at least on a smaller scale or in another combination elsewhere, but merging them will be highly challenging. Major limitations – as for any ESS instrument – could be the choppers placed close to the biological shielding in a very cramped space, the availability of large and economic area detectors with sufficient resolution, sensitivity and stability. Reducing the background from the source, our own beam optics and the neighbouring instruments needs a major effort.

HEIMDAL Technical Maturity	State of the art component	Potential Provider	Comments on manufacturing	Comments on risk management
Neutron guides				
Beam extraction multichannel guide and feeder for the thermal guide	Yes	SNAG Mirrotron	May be made on a metal guide	Radiation close to source
Thermal elliptic guide, m=max.5, L=160m, coating max m-5, optimized in the center to m=2-3	Yes	SNAG	Optimize coating M=5 (as less as acceptable)	accuracy
Thermal guide, mechanical support	No	SNAG		Lowe space at source region
Cold Guide, max M=2, M optimized, L=160m	Yes	SNAG	Standard	Standard
Cold guide, mechanical support	No	SNAG	Standard	Standard
Choppers (details see table II) inclusive electronics				
TC1, pulse shaping chopper, f=280Hz, R700=mm, counter-rotating disks	Yes	FZ/Astrium	Counterrotating Magnetic bearings	One motor versus source, needs space
TC2, pulse selection chopper, f=14Hz, R=700mm	No	FZ/Astrium		Synchronization to TC1 demanding
TC3, frame overlap chopper, f=14Hz, R=700mm	No	FZ/Astrium		Synchronization to TC1 demanding
CC1, band definition chopper, f=14Hz, R=600mm	No	FZ/Astrium		Synchronization to source
CC2, frame overlap chopper, f=14Hz, R=600mm	No	FZ/Astrium		Synchronization to CC1
CC2, frame overlap chopper, f=14Hz, R=600mm	No	FZ/Astrium		Synchronization to CC1
Detectors, detector electronics and radial collimators				
Cylindrical scintillation detector banks, left/right 1000mm high, R=1500mm, 30-175deg	Yes	PSI	Could be replaced by B development by ESS	Experience with POLDI@SINQ still in progress
Detector mechanics for cylindrical detector banks	No	TEL		
Additional backscattering detector unit, 1m x 0.5m, resolution 5mm	Yes	PSI	Restrictions in space due to guides	Experience with POLDI@SINQ
Radial collimator, 150 deg. 1000mm high, 1deg resolution	No	JJ SNAG		Standard, but large Low wavelengths
Mechanics for oscillating collimator	No	PSI JJ-Xray, SNAG	Standard - But large	

SANS PSD, 1 x 1.5 m, resolution < 2 x 5 mm	Yes	ESS	Boron ?	
SANS PSD Tank	No	TEL		Safety
SANS nose	No	TEL		
SANS protection booth, 8m long,3m high, 3m wide, air conditioned (outside of conventional building)	No	Locally		Temperature stability needed
Sample area, sample control area				
Vacuum box, shielding of sample area	No	TEL Trübbach	Safety aspects	Low permeability materials needed, motors !
xy stage for exact sample centering	No	Huber	Space, collision with IM camera to be solved	Low permeability materials needed, motors !
Instrument hutch and laboratory space	No	Locally		
Working platform for experiment access	No	Locally		Low permeability materials needed, motors !
Slits systems	No	Huber/JJ-Xray SNAG	Conflicts with guides restrict the space	Low permeability materials needed, motors !
Electronics and computing				
Instrument control electronic (without choppers and detectors)	Yes	ESS		
Local computing	Yes	ESS/DMCC	Multiple Rietveld necessary	
Shielding				
Instrument shielding	No	Hinneburg Alpha Beton	Low gamma level needed	Space vs. efficiency
shielding primary sector (part of ESS), 5 degrees	Yes	Hinneburg Alpha Beton	Weight vs accuracy Hinneburg for machining, Alpha Beton for raw products	Service, low space

2. LIST OF ABBREVIATIONS

Abbreviation	Explanation of abbreviation
APD	Avalanche-photo-diodes
CC	Cold chopper
DMSC	Data management and software center
DSC	Differential scanning calorimetry
IR	Infrared spectroscopy
NI	Neutron imaging
NPD	Neutron powder diffraction
PDF	Pair distribution function
Q	Scattering vector
SANS	Small angle neutron scattering
SAXS	Small angle X-ray scattering
SNAG	SwissNeutronics
Sr	steradian
TC	Thermal chopper
TG	Thermogravimetry
TS	Total scattering
TNPD	Thermal neutron powder diffraction
UV-VIS	Ultraviolet-visible spectroscopy
WAXS	Wide angle X-ray scattering

PROPOSAL HISTORY

New proposal:	(yes)
Resubmission:	(no)

References:

1. G. E. Moore, Cramming more components onto integrated circuits, Reprinted from Electronics, volume 38, number 8, April 19, 1965, pp.114 ff. *Solid-State Circuits Society Newsletter*, IEEE 11, 33-35 (2006).

2. L. Bjørn, The Skeptical Environmentalist: Measuring the Real State of the World. (Cambridge University Press, 1998).

3. G. Amow, S. J. Skinner, Recent developments in Ruddlesden-Popper nickelate systems for solid oxide fuel cell cathodes. *J. Solid State Electrochem.* 10, 538-546 (2006).

4. A. W. Hewat et al., High resolution neutron powder diffraction investigation of temperature and pressure effects on the structure of the high-Tc superconductor $Y_2Ba_4Cu_7O_{15}$. *Physica C: Superconductivity* 167, 579-590 (1990).

5. J. D. Grunwaldt, A. M. Molenbroek, N. Y. Topsoe, H. Topsoe, B. S. Clausen, In situ investigations of structural changes in Cu/ZnO catalysts. *Journal of Catalysis* 194, 452-460 (2000).

6. T. Kandemir et al., In situ neutron diffraction under high pressure-Providing an insight into working catalysts. *Nucl. Instrum. Methods Phys. Res. Sect. A-Accel. Spectrom. Dect. Assoc. Equip.* 673, 51-55 (2012).

7. B. S. Clausen et al., In situ cell for combined XRD and on-line catalysis tests: Studies of Cu-based water gas shift and methanol catalysts. *Journal of Catalysis* 132, 524-535 (1991).

8. A. Cervellino, J. Schefer, L. Keller, T. Woike, D. Schaniel, Identification of single photoswitchable molecules in nanopores of silica xerogels using powder diffraction. *Journal of Applied Crystallography* 43, 1040-1045 (2010).

9. S. L. S. Stipp et al., Behaviour of Fe-oxides relevant to contaminant uptake in the environment. Chemical Geology 190, 321-337 (2002).

10. B. C. Christiansen, T. Balic-Zunic, K. Dideriksen, S. L. S. Stipp, Identification of Green Rust in Groundwater. *Environmental Science & Technology* 43, 3436-3441 (2009).

11. M. Bremholm, M. Felicissimo, B. B. Iversen, Time-Resolved In Situ Synchrotron X-ray Study and Large-Scale Production of Magnetite Nanoparticles in Supercritical Water. *Angew. Chem.-Int. Edit.* 48, 4788-4791 (2009).

12. V. Middelkoop et al., Imaging the inside of a Continuous Nanoceramic Synthesizer under Supercritical Water Conditions Using High-Energy Synchrotron X-Radiation. *Chem. Mat.* 21, 2430-2435 (2009).

13. S. Takami et al., Neutron radiography on tubular flow reactor for hydrothermal synthesis: In situ monitoring of mixing behavior of supercritical water and room-temperature water. *Journal of Supercritical Fluids* 63, 46-51 (2012).

14. C. Tyrsted et al., Watching Nanoparticles Form: An In Situ (Small-/Wide-Angle X-ray Scattering/Total Scattering) Study of the Growth of Yttria-Stabilised Zirconia in Supercritical Fluids. *Chemistry – A European Journal*, 5759-5766 (2012).

15. R. A. Livingston, D. A. Neumann, A. J. Allen, S. A. Fitzgerald, R. Berliner, Application of neutron scattering to Portland cement. *Neutron News* 11, 18-24 (2000).

16. J. W. Phair, Green chemistry for sustainable cement production and use. *Green Chemistry* 8, 763-780 (2006).

17. M. P. Fang, P. E. Sokol, J. Y. Jehng, W. P. Halperin, Neutron Diffraction Study of Cement. *Journal of Porous Materials* 6, 95-99 (1999).

18. M. Castellote, C. Andrade, X. Turrillas, J. Campo, G. J. Cuello, Accelerated carbonation of cement pastes in situ monitored by neutron diffraction. *Cement and Concrete Research* 38, 1365-1373 (2008).

19. I. P. Swainson, E. M. Schulson, A neutron diffraction study of ice and water within a hardened cement paste during freeze–thaw. *Cement and Concrete Research* 31, 1821-1830 (2001).

20. P. J. McGlinn et al., Appraisal of a cementitious material for waste disposal: Neutron imaging studies of pore structure and sorptivity. *Cement and Concrete Research* 40, 1320-1326 (2010).

21. W. F. Kuhs, A. Klapproth, F. Gotthardt, K. Techmer, T. Heinrichs, The formation of meso- and macroporous gas hydrates. *Geophysical Research Letters* 27, 2929-2932 (2000).

22. W. F. Kuhs, T. C. Hansen, in Neutron Scattering in *Earth Sciences*, H. R. Wenk, Ed. (2006), vol. 63, pp. 171-204.

23. E. D. Sloan, Fundamental principles and applications of natural gas hydrates. *Nature* 426, 353-359 (2003).

24. M. A. Kelland, History of the development of low dosage hydrate inhibitors. *Energy Fuels* 20, 825-847 (2006).

25. B. Chazallon, W. F. Kuhs, In situ structural properties of N2-, O2-, and air-clathrates by neutron diffraction. *The Journal of Chemical Physics* 117, 308-320 (2002).

26. H. Ohno, I. Moudrakovski, R. Gordienko, J. Ripmeester, V. K. Walker, Structures of Hydrocarbon Hydrates during Formation with and without Inhibitors. *Journal of Physical Chemistry A* 116, 1337-1343 (2012).

27. D. K. Staykova, W. F. Kuhs, A. N. Salamatin, T. Hansen, Formation of porous gas hydrates from ice powders: Diffraction experiments and multistage model. *J. Phys. Chem. B* 107, 10299-10311 (2003).

28. M. Fiebig, Revival of the magnetoelectric effect. *J. Phys. D-Appl. Phys.* 38, R123-R152 (2005).

29. T. Lottermoser et al., Magnetic phase control by an electric field. *Nature* 430, 541-544 (2004).

30. M. Daraktchiev, G. Catalan, J. F. Scott, Landau theory of domain wall magnetoelectricity. *Physical Review B* 81, 224118 (2010).

31. M. Kenzelmann et al., Magnetic Inversion Symmetry Breaking and Ferroelectricity in $TbMnO_3$. *Physical Review Letters* 95, 087206 (2005).

32. H. Ohno, A window on the future of spintronics. *Nature Materials*, 9, 952–954 (2010).

33. Special issue Spintronics, *Nature Materials* 11, 353-476 (2012).

34. G. Catalan, J. F. Scott, A. Schilling, J. M. Gregg, Wall thickness dependence of the scaling law for ferroic stripe domains. *J. Phys.-Condes. Matter* 19, 022201 (2007).

35. G. Catalan et al., Fractal Dimension and Size Scaling of Domains in Thin Films of Multiferroic $BiFeO_3$. *Physical Review Letters* 100, 027602 (2008).

36. B. Ravel, M. P. Raphael, V. G. Harris, Q. Huang, EXAFS and neutron diffraction study of the Heusler alloy Co_2MnSi. *Physical Review B* 65, 184431 (2002).

37. J. M. DeTeresa et al., Evidence for magnetic polarons in the magnetoresistive perovskites. *Nature* 386, 256-259 (1997).

38. P. G. Radaelli et al., Mesoscopic and microscopic phase segregation in manganese perovskites. *Physical Review B* 63, 172419 (2001).

39. G. H. Rao et al., Magnetic phase transitions in Pr_5Ge_4. *Physical Review B* 69, 094430 (2004).

40. J. Seidel et al., Conduction at domain walls in oxide multiferroics. *Nature Materials* 8, 229-234 (2009).

41. E. A. Eliseev et al., Linear magnetoelectric coupling and ferroelectricity induced by the flexomagnetic effect in ferroics. *Physical Review B* 84, 174112 (2011).

42. K. P. Bhatti, S. El-Khatib, V. Srivastava, R. D. James, C. Leighton, Small-angle neutron scattering study of magnetic ordering and inhomogeneity across the martensitic phase transformation in $Ni_{50-x}Co_xMn_{40}Sn_{10}$ alloys. *Physical Review B* 85, 134450 (2012).

43. W. Kleemann, V. V. Shvartsman, P. Borisov, A. Kania, Coexistence of Antiferromagnetic and Spin Cluster Glass Order in the Magnetoelectric Relaxor Multiferroic $PbFe_{0.5}Nb_{0.5}O_3$. *Physical Review Letters* 105, 257202 (2010).

44. M. Bertelsen,GuideBot Software Package (2013)

45. N. J. Rhodes, Scientific Reviews: Status and Future Development of Neutron Scintillation Detectors. *Neutron News* 17, 16-18 (2006).

46. C. J. Schmidt, F. Groitl, M. Klein, U. Schmidt, W. Häussler, CASCADE with NRSE: Fast Intensity Modulation Techniques used in Quasielastic Neutron Scattering. *J. Phys., Conf. Ser.* 251, 012067 (2010).

47. http://medipix.web.cern.ch/medipix/pages/images.php